

# Assessment for WKBANSP 2024 using age-structured data in SS3: Anchovy in ICES Subdivision 9a South (ane.27.9a Southern component)

María José Zúñiga\*, Margarita María Rincón† Fernando Ramos‡

## Assessment model

The assessment of the anchovy in ICES division 9a, southern component was performed in Stock Synthesis software, version 3.30.22.1 (SS3, Methot *et al.*, 2024) under the Linux platform. SS3 is a generalized age and/or length-based model that is very flexible with regard to the types of data that may be included, the functional forms that are used for various biological processes, the level of complexity and number of parameters that may be estimated. The model is coded in C++ with parameter estimation enabled by automatic differentiation ([www.admb-project.org](http://www.admb-project.org)) and available at the NOAA Fisheries integrated toolbox: <https://noaa-fisheries-integrated-toolbox.github.io/SS3>. A description and discussion of the model can be found in Methot and Wetzel (2013).

The model is defined quarterly between 1989 and 2023, for one area and it is age-based, where the population is comprised of 3+ age-classes (with age 3 representing a plus group) with sexes combined (male and females are modelled together).

## Data

Input data include total catch (in biomass) and age composition of the catch (in proportion) for the commercial fleet (*SEINE*); abundance (in biomass) and age composition from three annual surveys: *PELAGO*, *ECOCADIZ* and *ECOCADIZ-RECLUTAS*; and spawning-stock biomass (SSB) estimates from a triennial DEPM *BOCADEVA* survey. To account for catches seasonality, the *SEINE* fleet have been divided into four fleets, one per quarter.

The Figure 1 provides a visual representation of the input data used in the model, categorized into three main types: catches, abundance indices, and age compositions. These data are displayed over time (years) and are represented by circles, with the size of each circle reflecting the magnitude of the data.

---

\*Centro Oceanográfico de Cádiz (COCAD-IEO), CSIC

†Centro Oceanográfico de Cádiz (COCAD-IEO), CSIC

‡Centro Oceanográfico de Cádiz (COCAD-IEO), CSIC

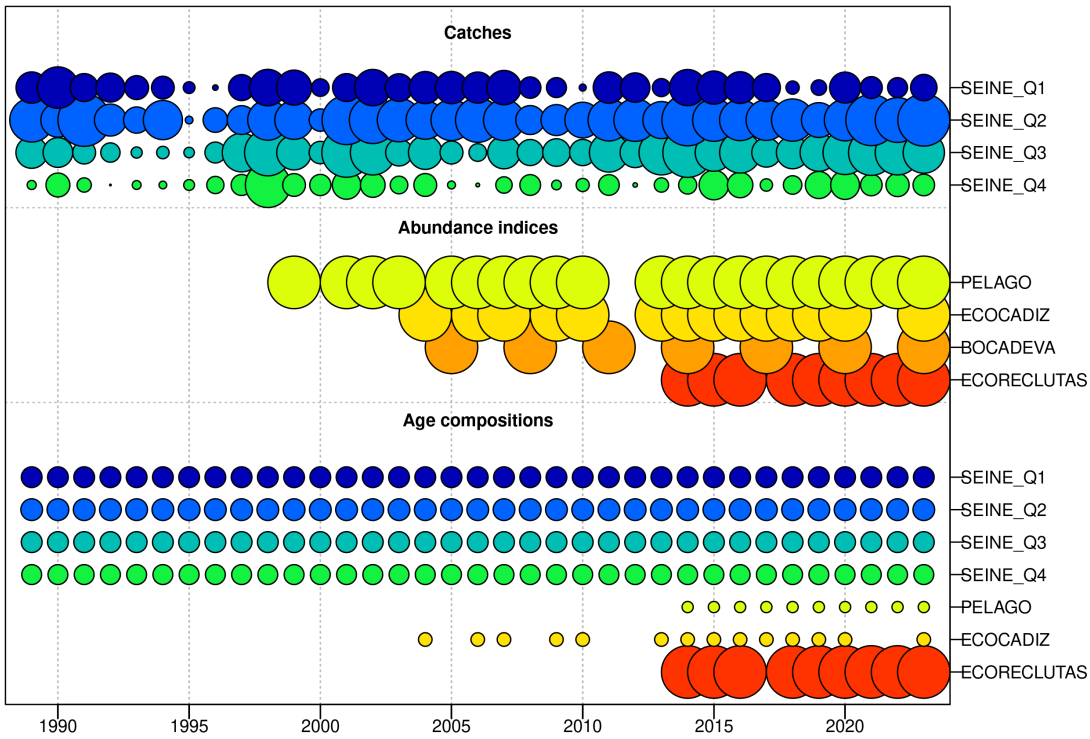


Figure 1: ane.27.9a Southern stock. Summary of model data input by year, where circle area is relative within a data type. Circles are proportional to total catch for catches, to precision for indices and to total sample size for age compositions.

## Catches

Anchovy catches in the Gulf of Cádiz exhibit seasonality, with 40.61% concentrated in the second quarter (Q2), averaging 2120.26 tons historically, followed by the third quarter (Q3) with 29.60% (1545.23 tons), the first quarter (Q1) with 19.39% (1012.42 tons), and the fourth quarter (Q4) with 10.39% (542.61 tons). In 2023, first-quarter catches were 7.84% lower than the historical average, while second, third, and fourth-quarter catches increased by 71.03%, 48.06%, and 14.70%, respectively (Figures 2 and 3).

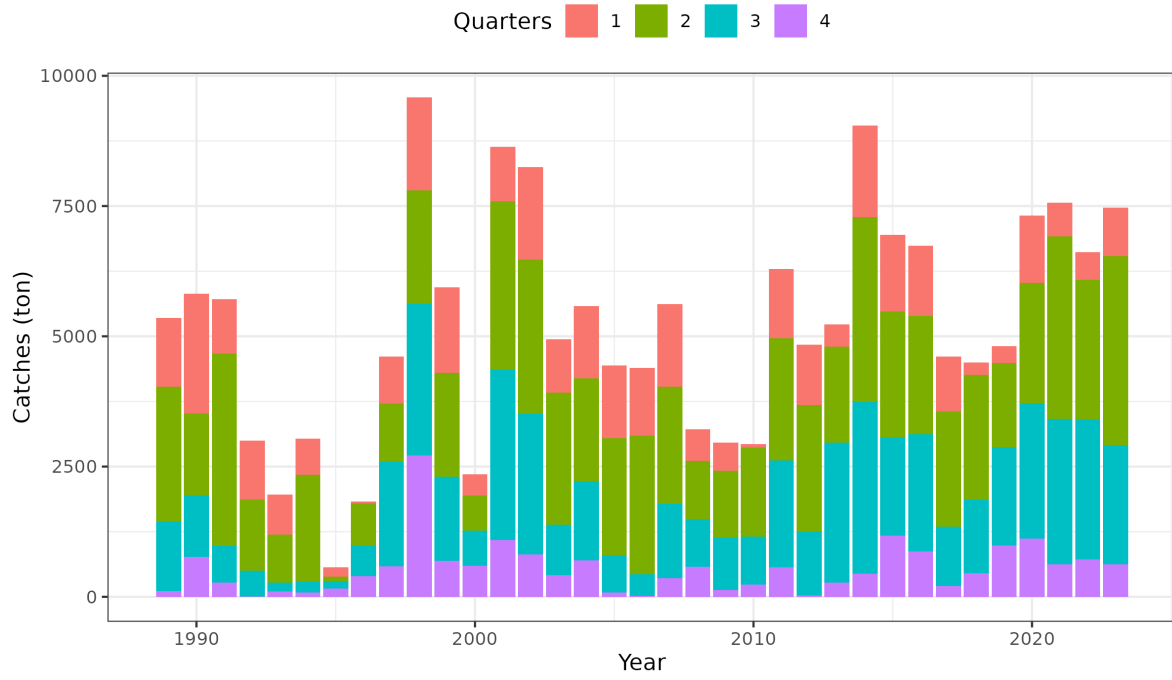


Figure 2: ane.27.9a Southern stock. Time series of quarterly catches.

Year	Catches (ton)				
	Q1	Q2	Q3	Q4	Total
1989	1318	2589	1336	111	5354
1990	2300	1571	1182	765	5818
1991	1049	3693	702	274	5718
1992	1125	1368	500	4	2997
1993	767	921	167	105	1960
1994	690	2055	210	80	3035
1995	185	80	148	157	570
1996	41	807	586	398	1832
1997	908	1110	2007	588	4613
1998	1781	2176	2909	2716	9582
1999	1638	1995	1616	691	5940
2000	412	668	673	600	2353
2001	1046	3227	3275	1089	8637
2002	1772	2957	2699	816	8244
2003	1027	2539	965	416	4947
2004	1384	1976	1522	699	5581
2005	1398	2252	706	85	4441
2006	1297	2657	416	19	4389
2007	1581	2251	1423	361	5616
2008	613	1121	910	576	3220
2009	533	1280	1016	126	2955
2010	67	1709	920	232	2928
2011	1326	2343	2051	571	6291
2012	1159	2433	1220	26	4838
2013	434	1837	2683	277	5231
2014	1754	3553	3300	439	9046
2015	1471	2425	1880	1174	6950
2016	1352	2267	2254	869	6742
2017	1051	2213	1140	206	4610
2018	236	2391	1414	458	4499
2019	322	1621	1889	982	4814
2020	1286	2315	2603	1113	7317
2021	644	3500	2794	623	7561
2022	532	2682	2679	722	6615
2023	933	3626	2288	622	7469

Figure 3: ane.27.9a Southern stock. Time series data of quarterly catches

## Abundance indices

The abundance indices *PELAGO*, *ECOCADIZ*, *BOCADEVA*, and *ECOCADIZ-RECLUTAS* exhibit inter-annual variability over time (Figure 4). *PELAGO*, with data from 1999 to 2023, shows fluctuations with a peak in 2016 at 65,345 tons, followed by a decline, but with a slight recovery in 2023 to 26,786 tons. *ECOCADIZ*, covering the period from 2004 to 2023, reaches its maximum in 2019 at 57,700 tons, followed by a significant decrease to 9,714 tons in 2023. *BOCADEVA*, with data from 2005 to 2023, shows a steady increase to its peak in 2020 at 81,466 tons, followed by a reduction to 15,138 tons in 2023. *ECOCADIZ-RECLUTAS*, recorded from 2014 to 2023, shows a sustained increase until 2019 at 48,398 tons, followed by a decrease to 8,300 tons in 2023.

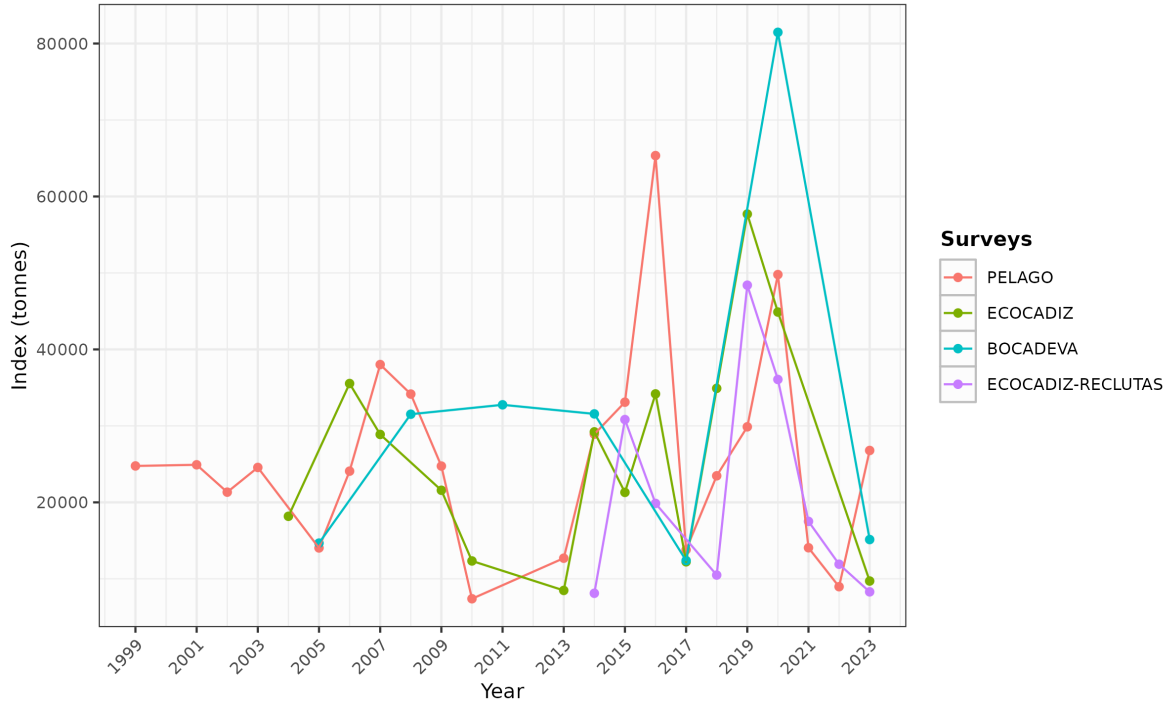


Figure 4: ane.27.9a Southern stock. Biomass estimates from *PELAGO*, *ECOCADIZ*, *BOCADEVA*, and *ECOCADIZ-RECLUTAS* surveys.

As it can be observed also in the raw data (Figure 5), these patterns reflect a high variability in abundance over time with periods of increase followed by declines in the later years of each series.

Acoustic Biomass (ton) by surveys				
year	PELAGO	ECOCADIZ	BOCADEVA	ECOCADIZ-RECLUTAS
1999	24763			
2001	24913			
2002	21335			
2003	24565			
2004		18177		
2005	14041		14673	
2006	24082	35539		
2007	38020	28882		
2008	34162		31527	
2009	24745	21580		
2010	7395	12339		
2011			32757	
2013	12700	8487		
2014	28917	29219	31569	8113
2015	33100	21305		30827
2016	65345	34184		19861
2017	13797	12229	12392	
2018	23473	34908		10493
2019	29876	57700		48398
2020	49787	44887	81466	36070
2021	14065			17512
2022	8972			11912
2023	26786	9714	15138	8300

Figure 5: ane.27.9a Southern stock. Acoustic biomass (ton) by surveys *PELAGO*, *ECOCADIZ*, *BOCADEVA*, and *ECOCADIZ-RECLUTAS*.

## Age composition

In the model, the age proportion of the commercial fleet (*SEINE*) by quarter from 1989 to 2023, is used (Figure 6). It can be observed that age-0 proportion compared to other ages has been increasing in the last years while age-1 predominates in Q1 and Q2, with a constant proportion over time. Age-0 is not recorded in Q1 and Q2 by convention. In Q3 and Q4, the proportion of age-1 individuals decreases as the proportion of age-0 increases. Additionally, ages 2 and 3 exhibit lower and variable proportions across all quarters over the years, without a defined pattern of change.

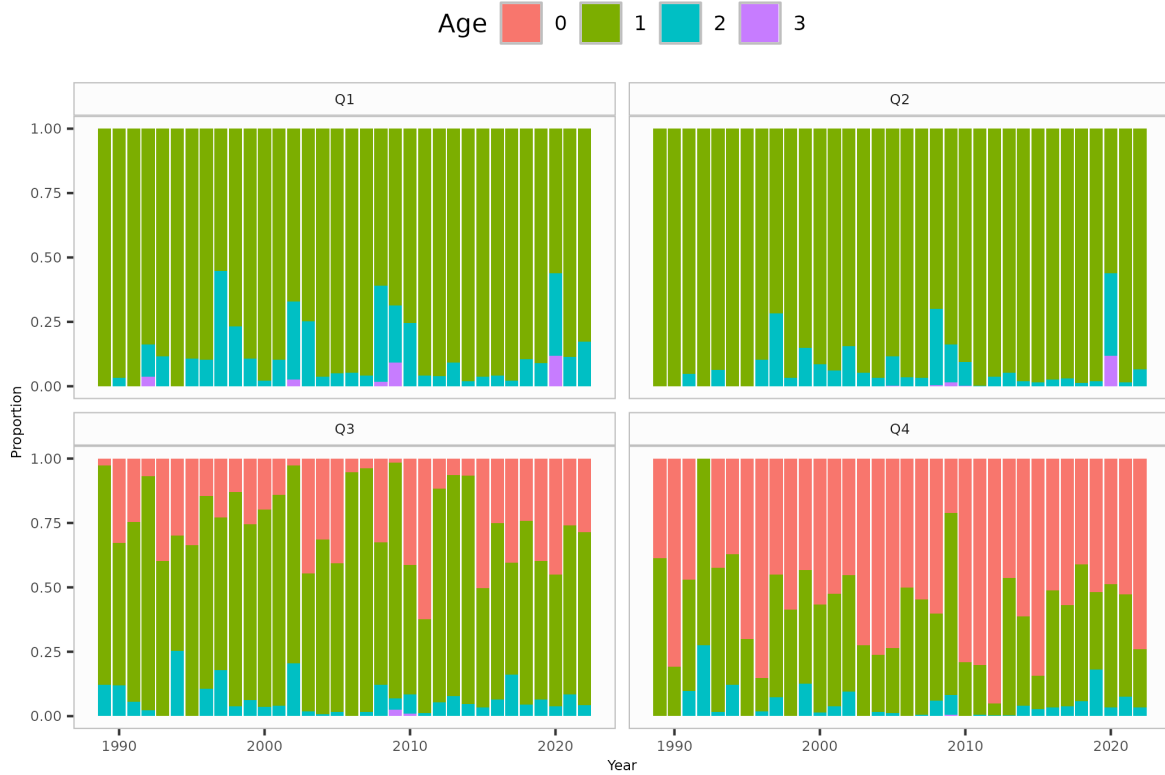


Figure 6: ane.27.9a Southern stock. Age proportion in the commercial fleet catches (*SEINE*) by quarter (1989 to 2023).

Figure 7 shows the yearly age proportions from surveys *PELAGO*, *ECOCADIZ*, and *ECOCADIZ-RECLUTAS* that were used as input for the model. It can be observed that in the *PELAGO* survey, conducted in the second quarter (Q2), age 1 represents the highest proportion over time, with a presence of ages 2 and 3, and no records of age 0 individuals. The *ECOCADIZ* survey, primarily conducted in the third quarter (Q3), shows a predominance of age 1, with an increase in the proportion of age 0 from 2010 onwards; in 2004 and 2006, when the survey was conducted in the second quarter (Q2), no age 0 individuals were recorded by convention. The *ECOCADIZ-RECLUTAS* survey, conducted since 2014 in October (fourth quarter, Q4), shows a higher proportion of age 0, followed by age 1, with lower representation of ages 2 and 3.

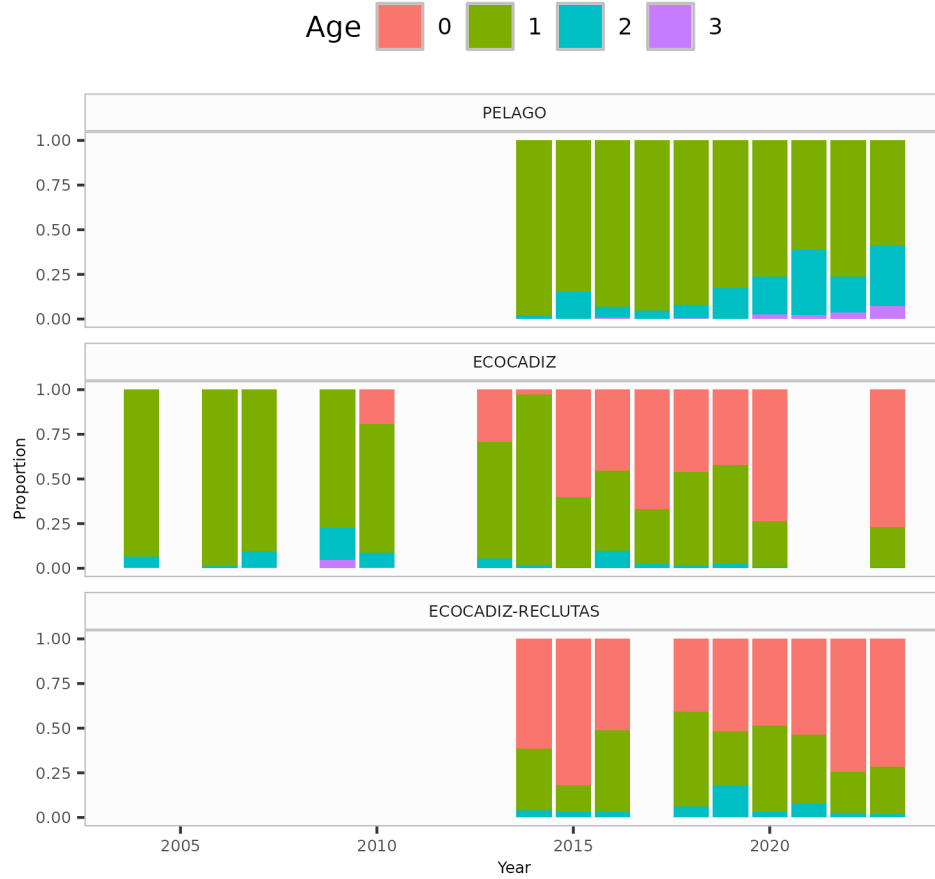


Figure 7: ane.27.9a Southern stock. Age proportion in acoustic surveys estimates (*PELAGO*, *ECOCADIZ*, and *ECOCADIZ-RECLUTAS*).

## Weigth-at-age

Figure 8 presents the age-specific weight-at-age values at the start of each season, estimated from external data sources. The figure illustrates that mean weight differences between age groups remain consistent over time, with some variability observed across quarters. Individuals aged 3 show greater variability in mean weight compared to younger age groups. For further details, refer to the working document by **Zuñiga et al. (2024)**.

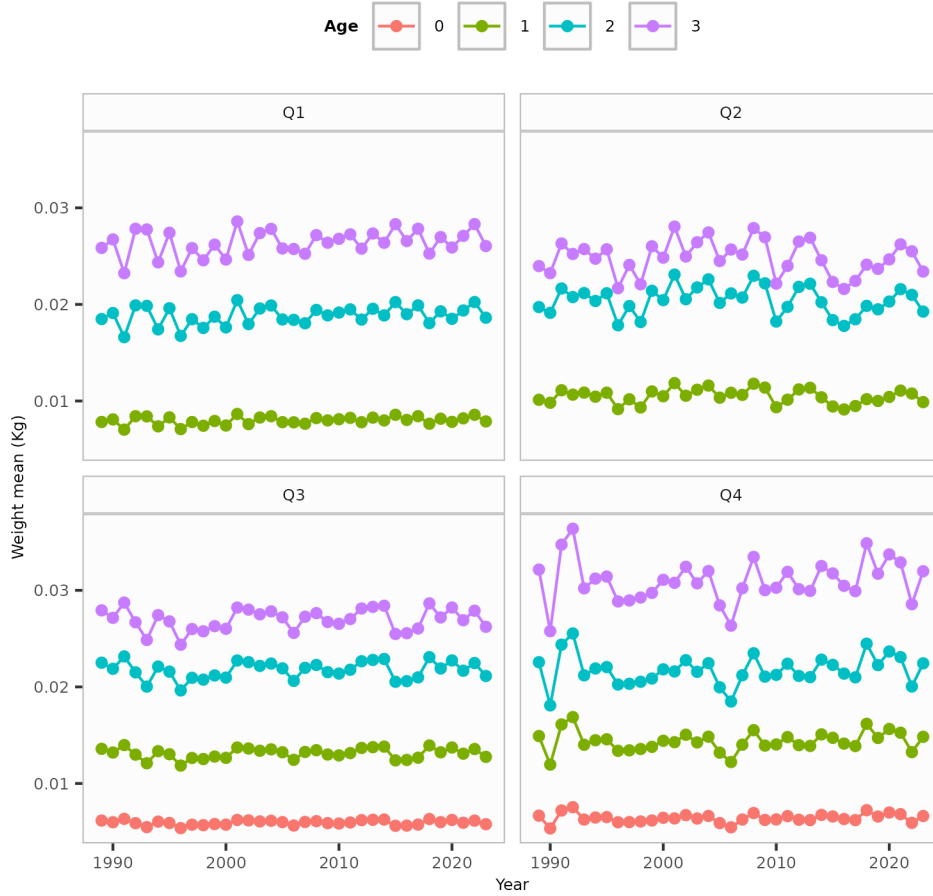


Figure 8: ane.27.9a Southern stock. Weight at age by quarters.

## Model settings

### Natural mortality

Age-specific natural mortality input values at the beginning of the year were derived from external data sources. For further details, refer to the working document by **Rincón et al. (2024)**.

Parameter	Age_0	Age_1	Age_2	Age_3
natM1	2.97	1.33	1.33	1.33

### Maturity

Due to some inconsistencies in the maturity ogives not noticed during WKPELA 2018, we assume that all individuals with age 1 or higher ( $B_{1+}$ ), are mature i.e. these abundance estimates result equivalent to spawning stock biomass ( $SSB$ ) estimates. For further details, refer to the working document by **ICES 2024** and **WD Rincón et al. (2024)**.

Parameter	Age_0	Age_1	Age_2	Age_3
Maturity	0	1	1	1

## Growth

It is not modelled explicitly.

## Recruitment

Equilibrium recruitment ( $R_0$ ) was estimated in the base model, and steepness (h) was fixed at 0.8. The initial steepness estimate is based on values reported by Hsu *et al.* (2024), with a mean of 0.82 and a range of 0.59 to 0.93, and by Wiff *et al.* (2018), who reported steepness values between 0.58 and 0.86 for pelagic species. Standard deviation of log number of recruits was set to 0.6.

The early recruitment deviations for the initial population were estimated for the period 1985-1988. A recruitment bias adjustment ramp (Methot and Taylor, 2011) was applied to this early period, and bias-adjusted recruitment was estimated for the main period. Recruitment deviations for the main period were estimated for 1991-2023.

## Fishing mortality

Calculation of fishing mortality is performed by using the hybrid F method that does a Pope's approximation to provide initial values for iterative adjustment of the Baranov continuous F values to closely approximate the observed catch. Total catch biomass by year is assumed to be accurate and precise and the F values are tuned to match this catch.

## Catchability

All the surveys are assumed to be relative indices of abundance. The catchability is modelled with a simple  $q$  linear model.

## Selectivity

The fishery and the surveys selectivity were defined as logistic functions fixed over time. Nevertheless, considering the difference in age patterns over the years in the *ECOCADIZ* survey it was decided to split it into two periods: 2004-2014 and 2015-2023.

## Data weighting

Constant standard errors of 0.05 and 0.3 were assumed for quarterly catches and surveys, respectively.

The age compositions were adjusted assuming a multinomial error structure with variance described by the sample size, set at 100 for both, the commercial fleet and acoustic surveys. After that, these data was weighted using the Francis method TA1.8 (Francis, 2011).

## Initial population

It is calculated by estimating an initial equilibrium population modified by age composition data in the first year of the assessment (Methot and Wetzel, 2013). The model starts in 1988 and the equilibrium population age structure was assumed to be in an exploited state with an initial catch of 0 tonnes

Variance estimates for all estimated parameters are calculated from the Hessian matrix. Minimisation of the likelihood is implemented in phases using standard ADMB process. The phases in which estimation will begin for each parameter are shown in the control file available in the TAF repository for this stock ([https://github.com/ices-taf/2024\\_ane.27.9a\\_south\\_benchmark](https://github.com/ices-taf/2024_ane.27.9a_south_benchmark)). The R packages r4ss version 1.50.0 (Taylor *et al.*, 2021) and ss3diags version 1.10.3 (Carvalho *et al.*, 2021) were used to process and view model outputs. All analyses were conducted in R version 4.4.1 (2024-06-14).

## Diagnostics

The model successfully converged, as evidenced by the Hessian matrix being positive definite and the final gradient being relatively small, with a gradient value of 0.0000088. The “Status” column in Figure 9 shows that the initial model configuration has allowed for adequate optimization of the parameters. Additionally, the gradient for all parameters is relatively small. It is important to note that the bounds imposed on the initial parameters have not restricted the search for optimized values, as reflected in the “Afterbound” column.

Parameter	Value	Phase	Min	Max	Init	Status	Parm_StDev	Gradient	Afterbound
SR_LN(R0)	15.537300	1	1.0	25.0	20.0	OK	0.0202286	-0.000002902400000	OK
LnQ_base_PELAGO(5)	1.181530	2	-30.0	15.0	0.0	OK	0.3354880	-0.000001285890000	OK
LnQ_base_ECOCADIZ(6)	1.339300	2	-30.0	15.0	0.0	OK	0.4701520	0.000000727476000	OK
LnQ_base_BOCADEVA(7)	1.847040	2	-30.0	15.0	0.0	OK	0.1251790	-0.000004784390000	OK
LnQ_base_ECORECLUTAS(8)	1.841860	1	-30.0	15.0	0.0	OK	0.2498140	0.000005941930000	OK
Age_inflection_SEINE_Q1(1)	0.930026	2	0.0	4.0	0.0	OK	0.7851080	-0.000001562900000	OK
Age_95%width_SEINE_Q1(1)	0.198602	2	0.1	0.3	0.2	OK	2.2253600	-0.000000027394300	OK
Age_inflection_SEINE_Q2(2)	0.194172	2	0.1	0.3	0.2	OK	2.2129800	0.000000000998684	OK
Age_95%width_SEINE_Q2(2)	0.206624	2	0.0	4.0	0.5	OK	2.1450700	-0.000000005568720	OK
Age_inflection_SEINE_Q3(3)	0.229521	2	0.0	4.0	0.0	OK	1.3760200	0.000000201413000	OK
Age_95%width_SEINE_Q3(3)	0.187959	2	0.0	4.0	0.5	OK	1.1268200	-0.000000204574000	OK
Age_inflection_SEINE_Q4(4)	0.463384	2	0.0	4.0	0.0	OK	0.2558520	-0.000001398380000	OK
Age_95%width_SEINE_Q4(4)	0.663873	2	0.0	4.0	0.5	OK	0.3095230	0.000001252340000	OK
Age_inflection_PELAGO(5)	0.893223	2	0.0	3.5	0.9	OK	1.4557100	0.000000395900000	OK
Age_95%width_PELAGO(5)	0.246366	2	0.1	0.4	0.3	OK	3.3392600	0.000000014853800	OK
Age_inflection_ECOCADIZ(6)	0.413031	3	-2.0	3.5	0.0	OK	2.8691000	-0.000006196260000	OK
Age_95%width_ECOCADIZ(6)	0.372468	3	-2.0	3.5	0.2	OK	2.5301900	0.000006984250000	OK
Age_inflection_ECORECLUTAS(8)	0.953594	2	-2.0	3.5	0.0	OK	0.1666880	-0.000003069310000	OK
Age_95%width_ECORECLUTAS(8)	1.043370	3	-2.0	3.5	1.0	OK	0.1011620	0.000004294120000	OK

Figure 9: ane.27.9a Southern stock. Parameters estimated by the initial base model.

## Model fit and residuals

The Figure 10 shows that the abundance indices from the acoustic surveys exhibit a high level of variability, as reflected by the width of the assumed confidence intervals, with a maximum coefficient of variation of 30%. The model follows the overall trend of the indices, though it encounters some difficulties in accurately fitting the extreme biomass values, both the highest and lowest. However, it adequately reproduces the general trend of variability in biomass levels presented by the survey estimates.

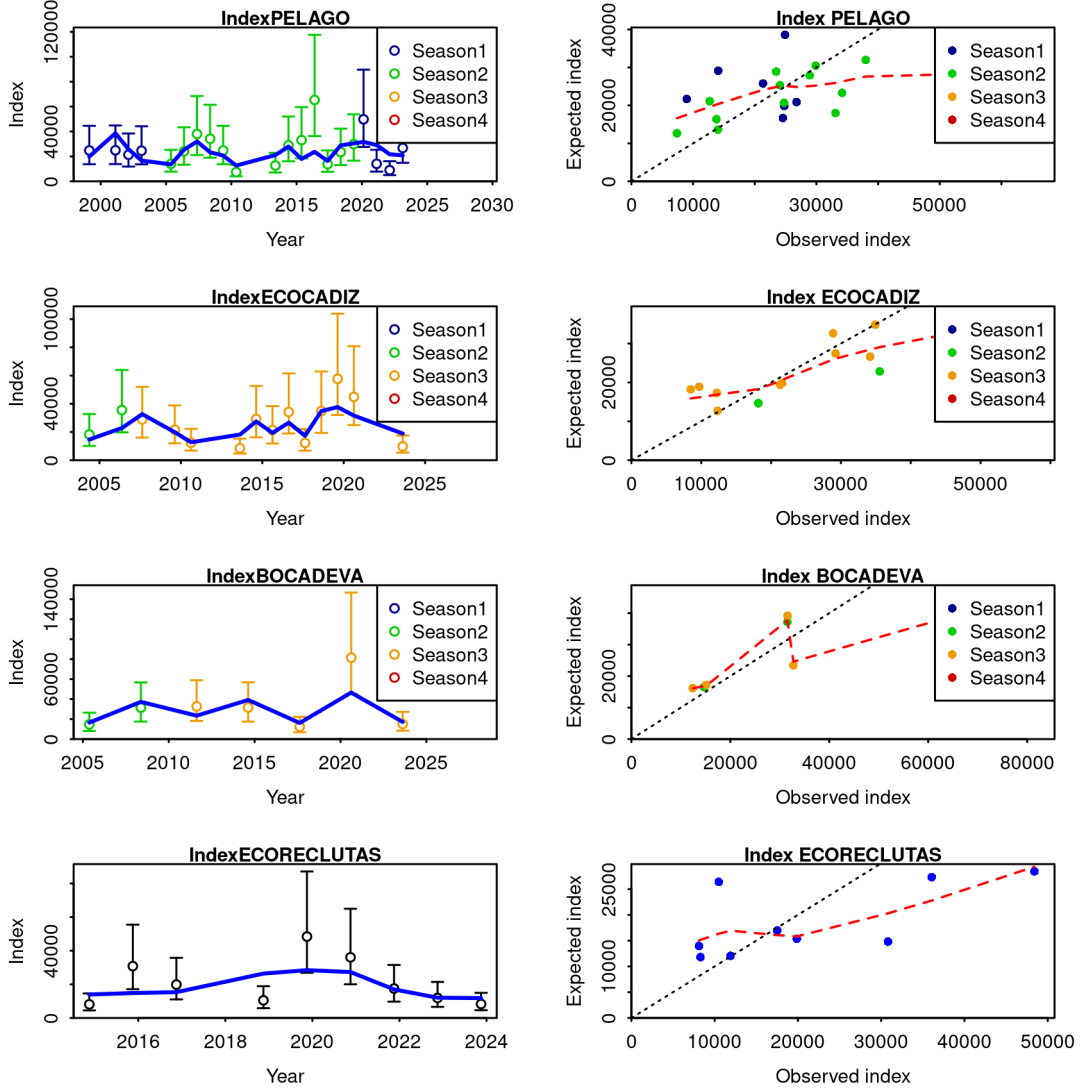


Figure 10: ane.27.9a Southern stock. Model fit to the data (left panel) and observed versus expected values (right panel) of the indices from the surveys *PELAGO*, *ECOCADIZ*, *BOCADEVA* and *ECOCADIZ-RECLUTAS*. The lines indicate a 95% uncertainty interval around the index values based on the lognormal error model assumption.

Figure 11 shows that the residuals from the fit of the biomass indices are randomly distributed, with p-values greater than 0.05 (*PELAGO* = 0.415, *ECOCADIZ* = 0.636, *BOCADEVA* = 0.888, *ECOCADIZ-RECLUTAS* = 0.374). The estimated root mean square error (RMSE) for the joint residual analysis is 41.7%.

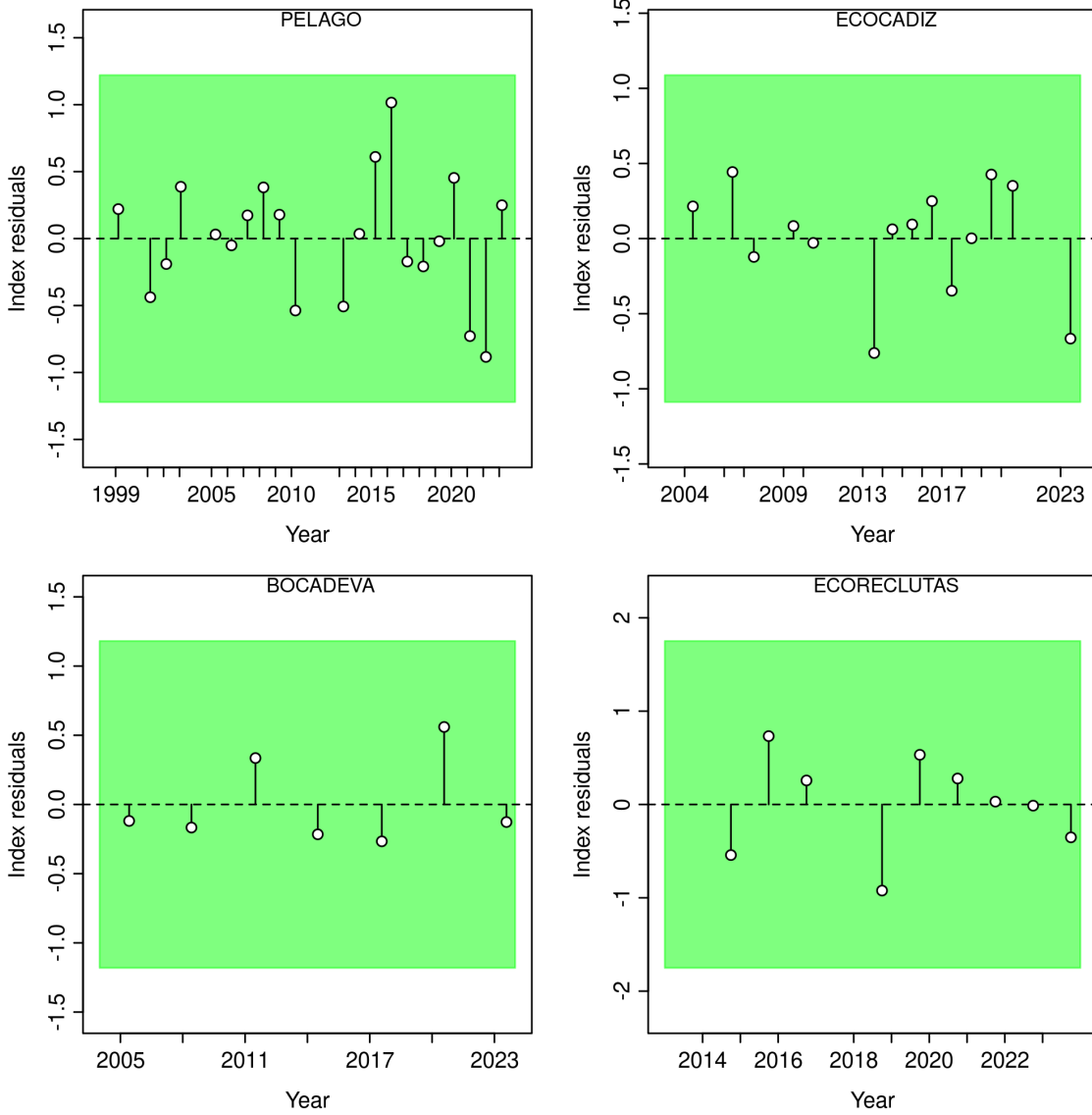


Figure 11: ane.27.9a Southern stock. a) Run test plots for the fit of acoustic and DEPM survey indices. Green shading indicates no evidence ( $p \geq 0.05$ ) and red shading indicates evidence ( $p < 0.05$ ) for rejecting the hypothesis of a randomly distributed residual time series, respectively. The shaded area (green/red) spans three standard residual deviations on either side of zero, and red points outside the shading violate the three-sigma limit for that series. b) Joint residual plots for the fit of acoustic and DEPM survey indices (bottom left panel). Vertical lines with points show the residuals, and the solid black line show loess smoother through all residuals. Boxplots indicate the median and quantiles in cases where residuals from multiple indices are available for a given year, with the solid black line showing a loess smoother. The root mean square error (RMSE) is included in the top right corner of the panel.

Estimated mean age for the *SEINE* fleet (one by quarter) with a 95% confidence intervals based on current sample sizes, is presented in Figure 12.

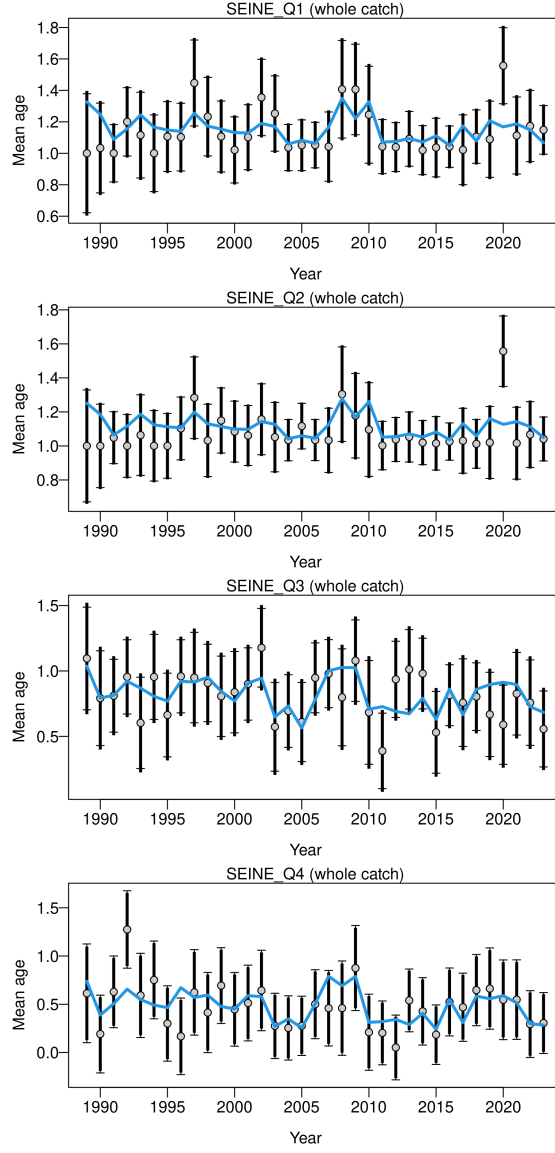


Figure 12: Mean age for commercial fleet by quarters with 95% confidence intervals based on current sample sizes. Francis data weighting method TA1.8: thinner intervals (with capped ends) show the result of further adjusting sample sizes based on the suggested multiplier (with 95% interval) for age data. The blue line corresponds to the estimated mean age.

While mean age for the *PELAGO*, *ECOCADIZ* and *ECOCADIZ-RECLUTAS* surveys is presented in Figure 13.

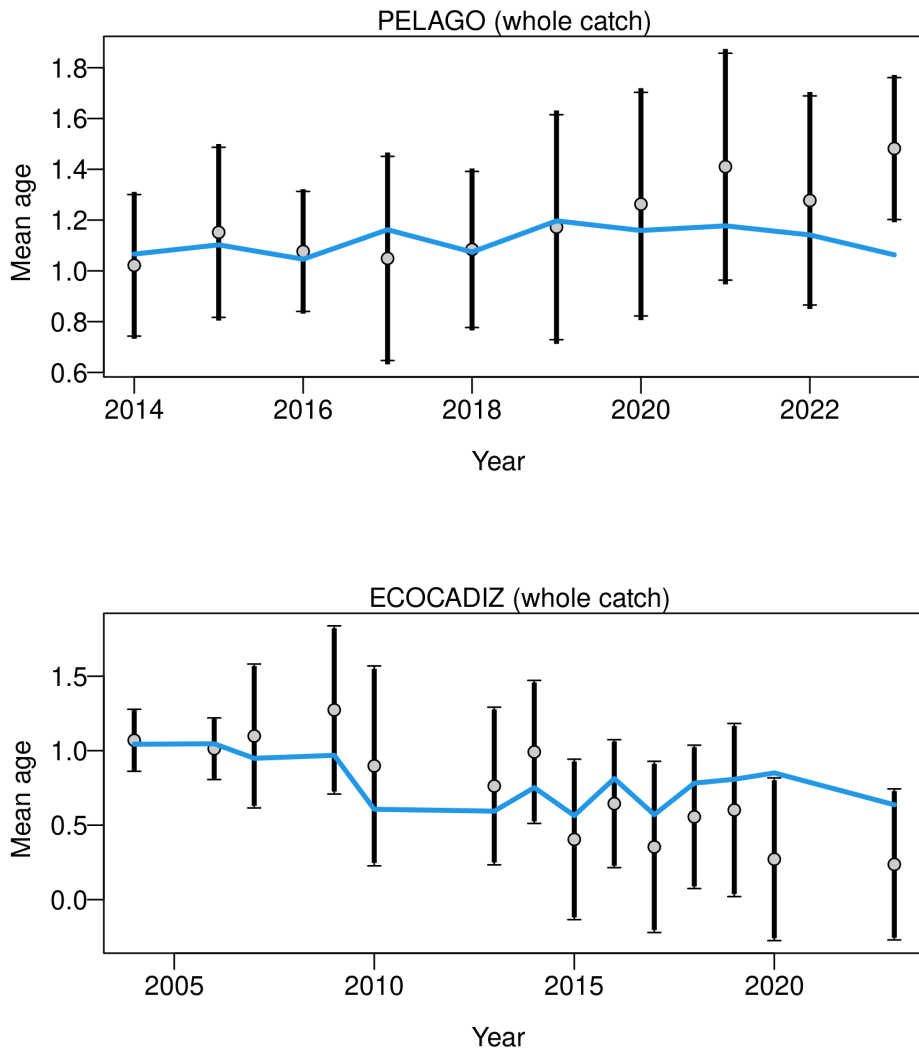


Figure 13: Mean age for *PELAGO*, *ECOCADIZ*, and *ECOCADIZ-RECLUTAS* with 95% confidence intervals based on current sample sizes. Francis data weighting method TA1.8: thinner intervals (with capped ends) show the result of further adjusting sample sizes based on the suggested multiplier (with 95% interval) for age data. The blue line corresponds to the estimated mean age.

The Figure 14 shows the estimated age compositions aggregated over time for the different age data sources: *SEINE*, *ECOCADIZ*, *PELAGO*, and *ECORECLUTAS*. Overall, a high proportion of young individuals (ages 0 and 1) is observed in both the commercial fleet catches and acoustic surveys, with a significant decline in the proportions of older age classes. The green lines represent the model fits, demonstrating an adequate fit, with the aggregated age compositions well reconstructed.

### Age comps, aggregated across time by fleet

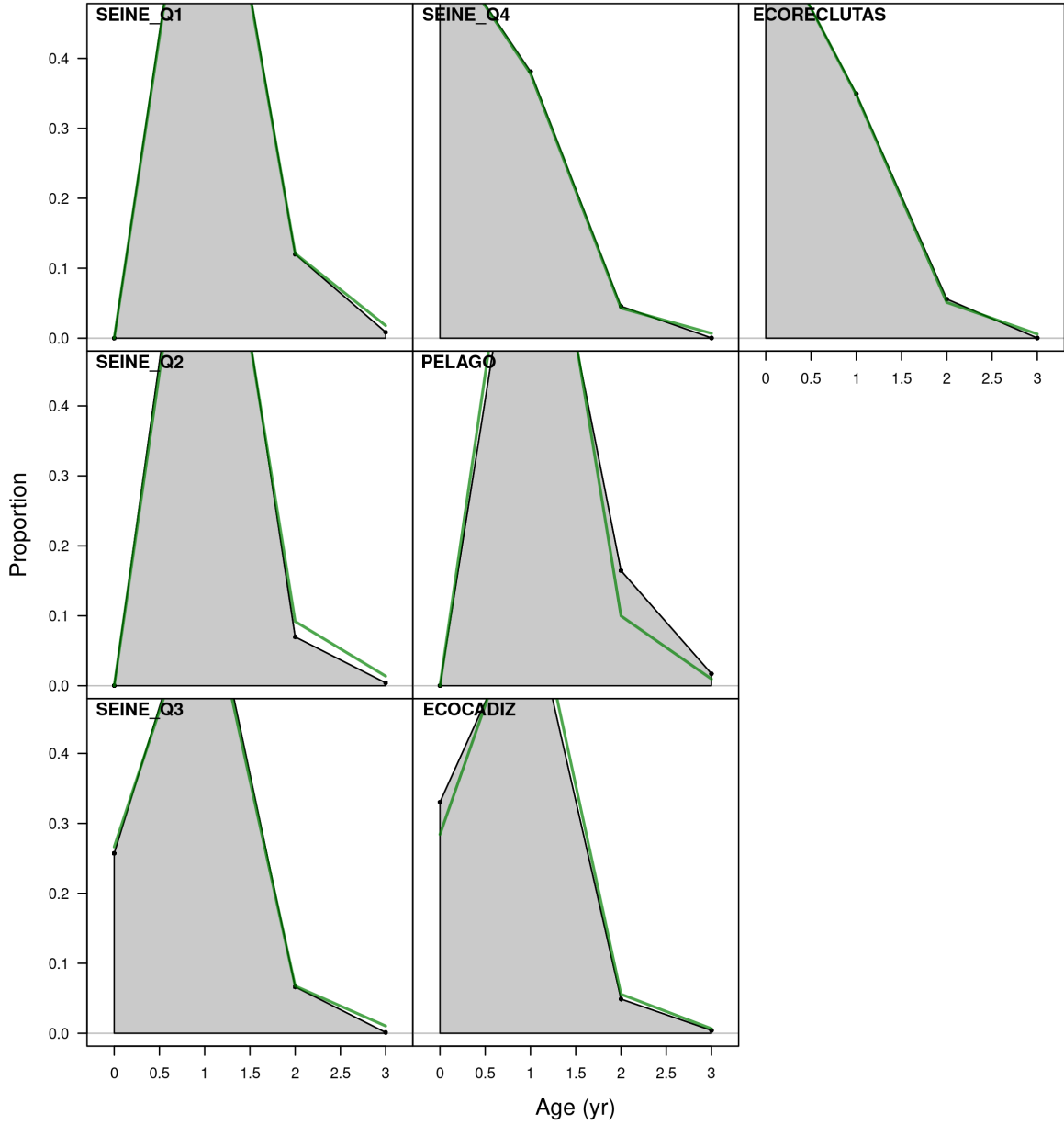


Figure 14: ane.27.9a Southern stock. Model fit to the aggregated age composition data from the *SEINE* fishery, and the acoustic surveys *PELAGO*, *ECOCADIZ*, and *ECOCADIZ-RECLUTAS*. The green line represents the model estimates, while the shaded grey area shows the observed data.

Figure 15 shows the estimated age composition for the commercial fleet in the first quarter.

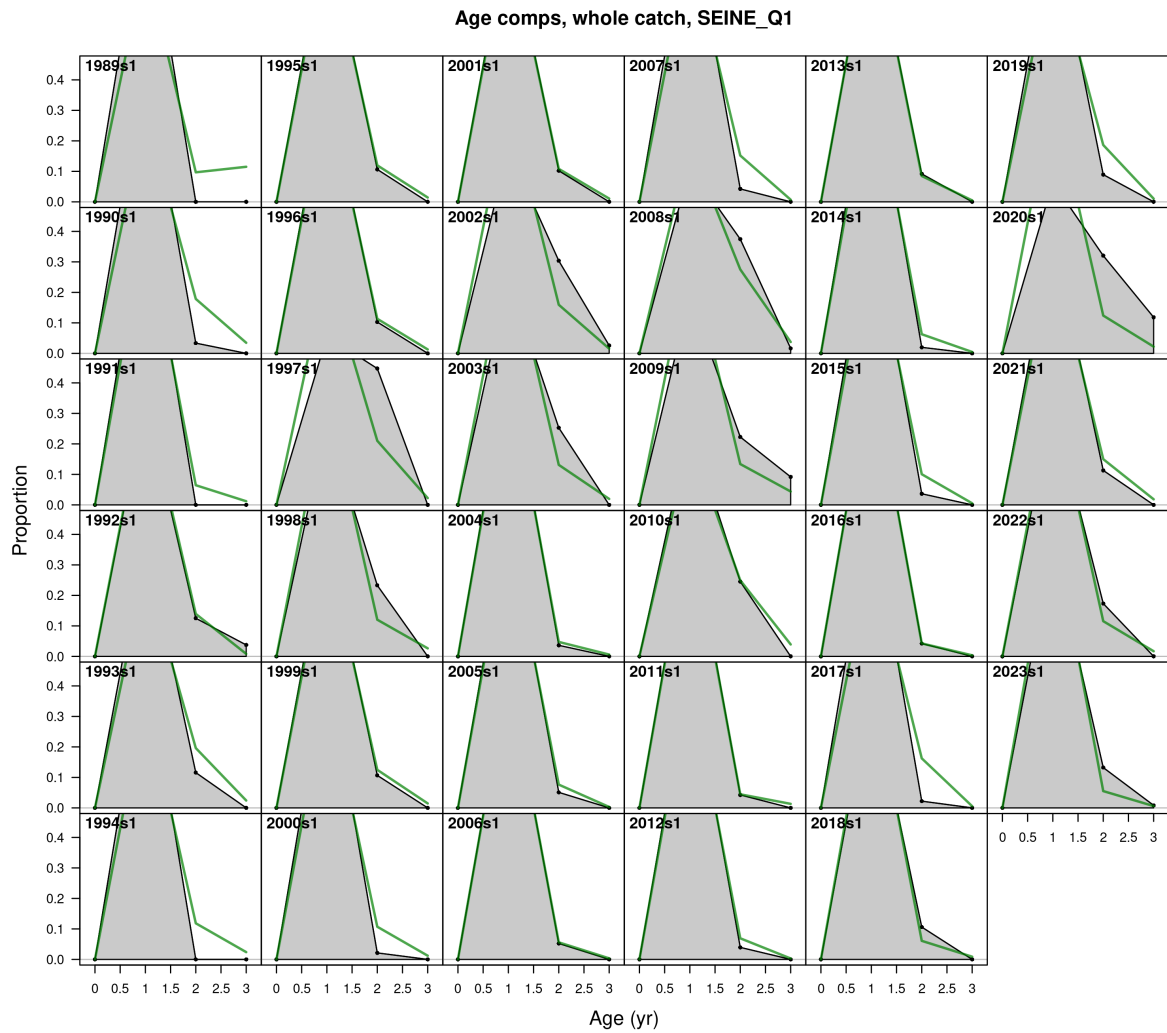


Figure 15: ane.27.9a Southern stock. Model fit to the age composition data from the *SEINEQ1* fishery, by year and quarter. The green line represents the model estimates, while the shaded grey area shows the observed data.

Figure 16 shows the estimated age composition for the commercial fleet in the second quarter.

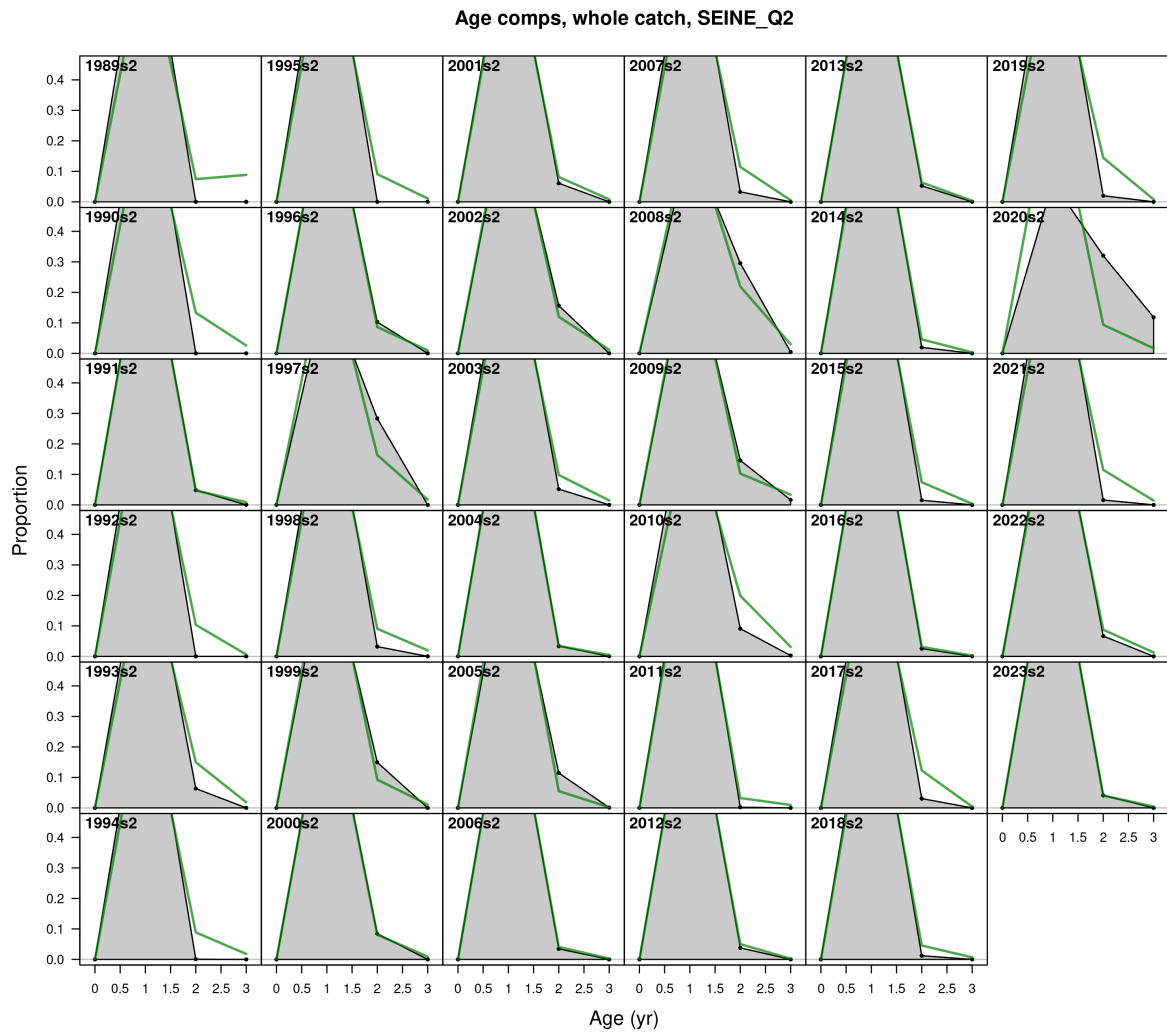


Figure 16: ane.27.9a Southern stock. Model fit to the age composition data from the *SEINEQ2* fishery, by year and quarter. The green line represents the model estimates, while the shaded grey area shows the observed data.

Figure 17 shows the estimated age composition for the commercial fleet in the third quarter.

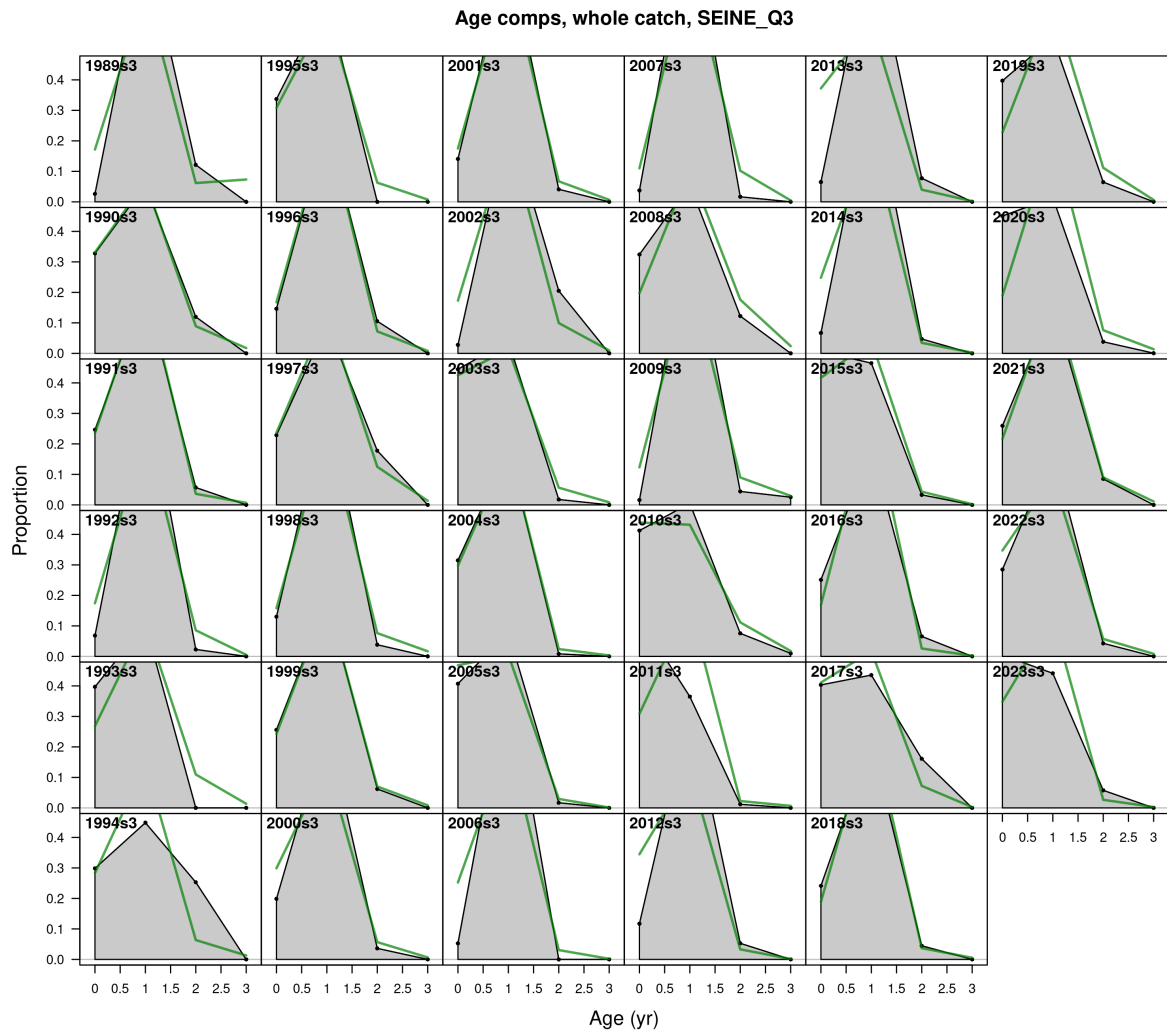


Figure 17: ane.27.9a Southern stock. Model fit to the age composition data from the *SEINEQ3* fishery, by year and quarter. The green line represents the model estimates, while the shaded grey area shows the observed data.

Figure 18 shows the estimated age composition for the commercial fleet in the fourth quarter.

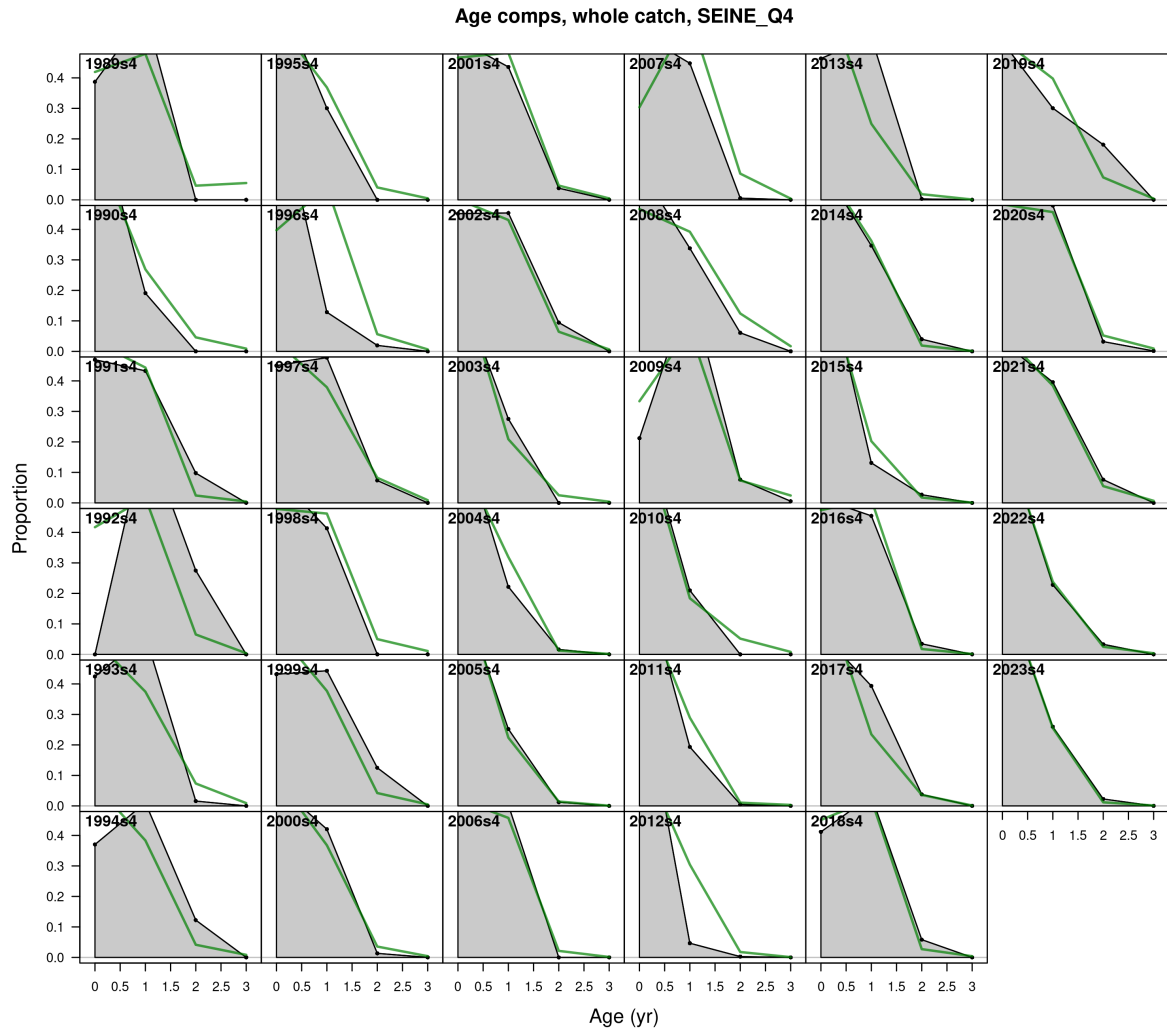


Figure 18: ane.27.9a Southern stock. Model fit to the age composition data from the *SEINEQ4* fishery, by year and quarter. The green line represents the model estimates, while the shaded grey area shows the observed data.

Although the aggregated fits show an overall adequate result, some years exhibit variability in the age composition of the commercial fleet (*SEINE*) catches. This pattern is also evident in the annual data fits for the *PELAGO* survey, especially in the later years of the series (2020-2023), where there is a tendency to overestimate age 1 and underestimate age 2 (Figure 19).

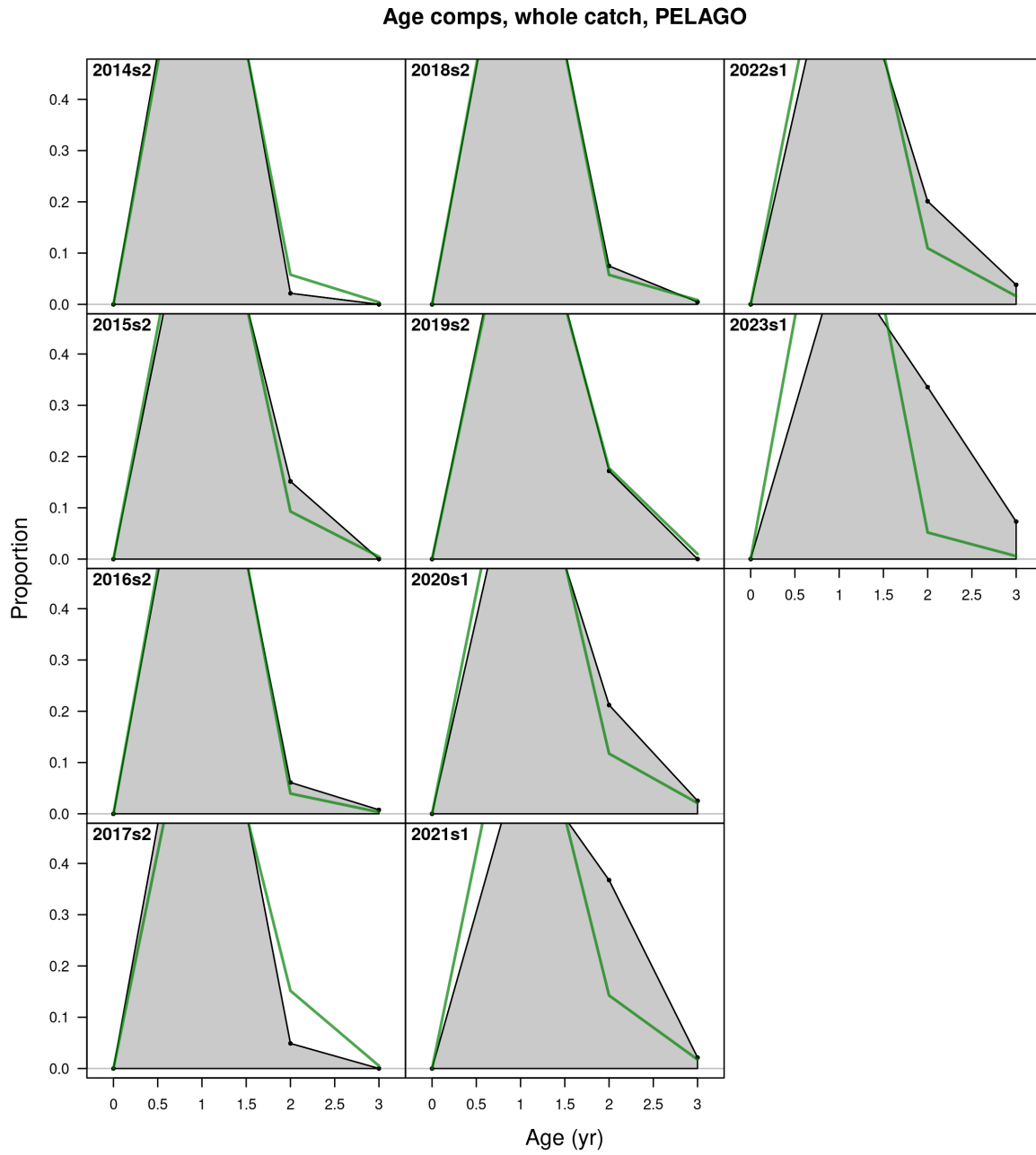


Figure 19: ane.27.9a Southern stock. Model fit to the age composition data from the *PELAGO* spring survey by year. The green line represents the model estimates, while the shaded grey area shows the observed data.

In the *ECOCADIZ* survey, there are difficulties in estimating ages 0 and 1, with a tendency to underestimate age 0 and overestimate age 1 from 2016 to 2023 (Figure20).

### Age comps, whole catch, ECOCADIZ

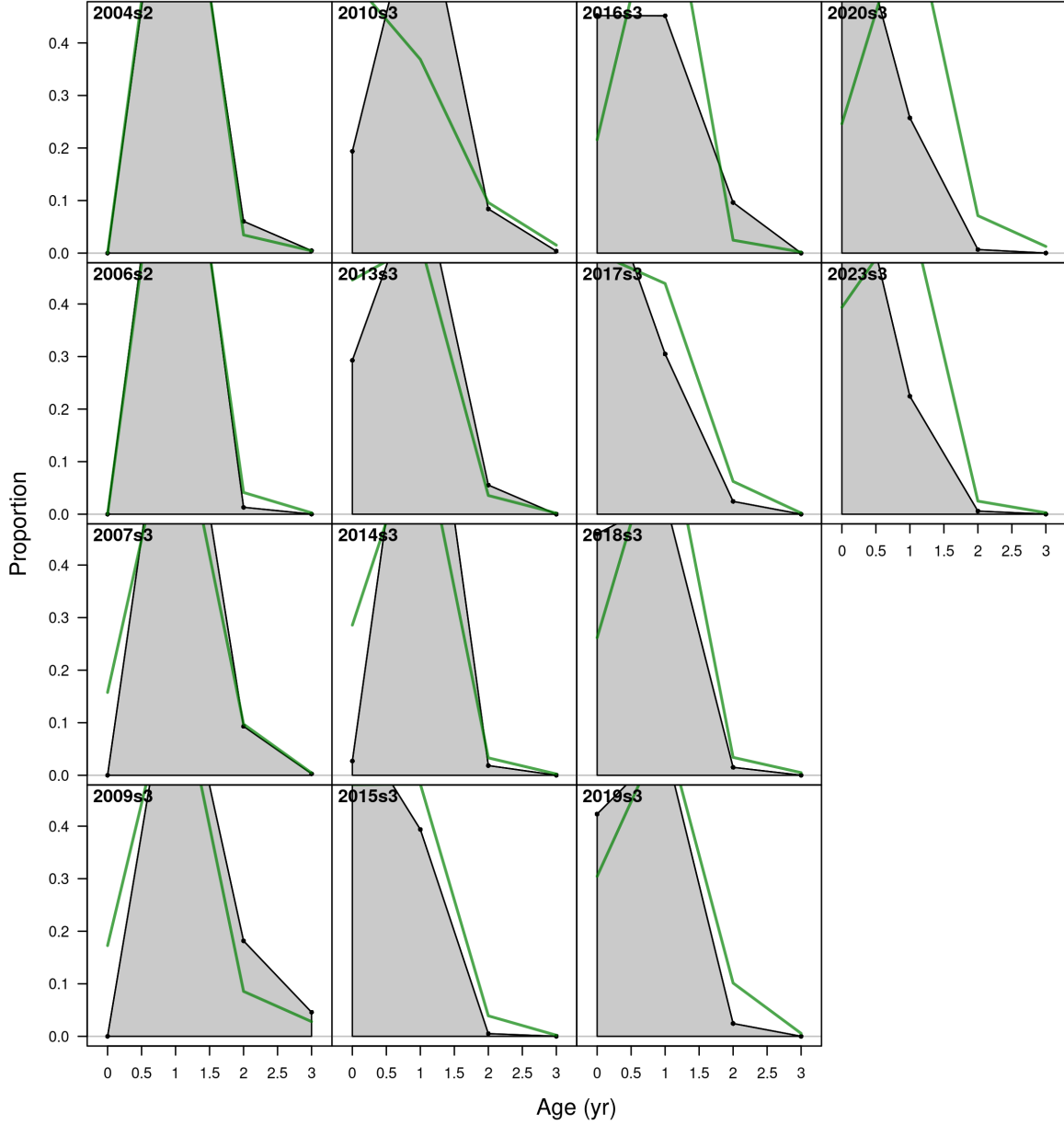


Figure 20: ane.27.9a Southern stock. Model fit to the age composition data from the *ECOCADIZ* summer survey by year. The green line represents the model estimates, while the shaded grey area shows the observed data.

In *ECOCADIZ-RECLUTAS*, a generally good fit is observed without a clear pattern of overestimation or underestimation (Figure 21).

Bubble plots of the residuals corresponding to the fit of the *SEINE* data are presented in Figure 21.

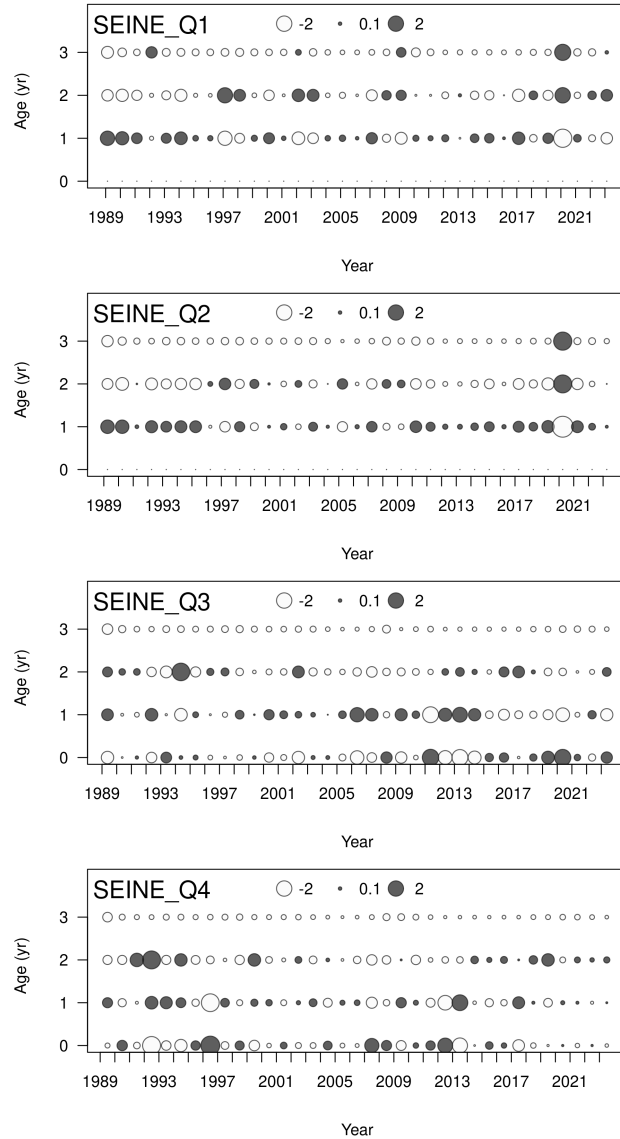


Figure 21: ane.27.9a Southern stock. Pearson residuals, comparing across fleets. Closed bubbles are positive residuals (observed > expected) and open negative residuals (observed < expected).

Bubble plots of the residuals corresponding to the fit of the surveys age-data are presented in Figure 22.

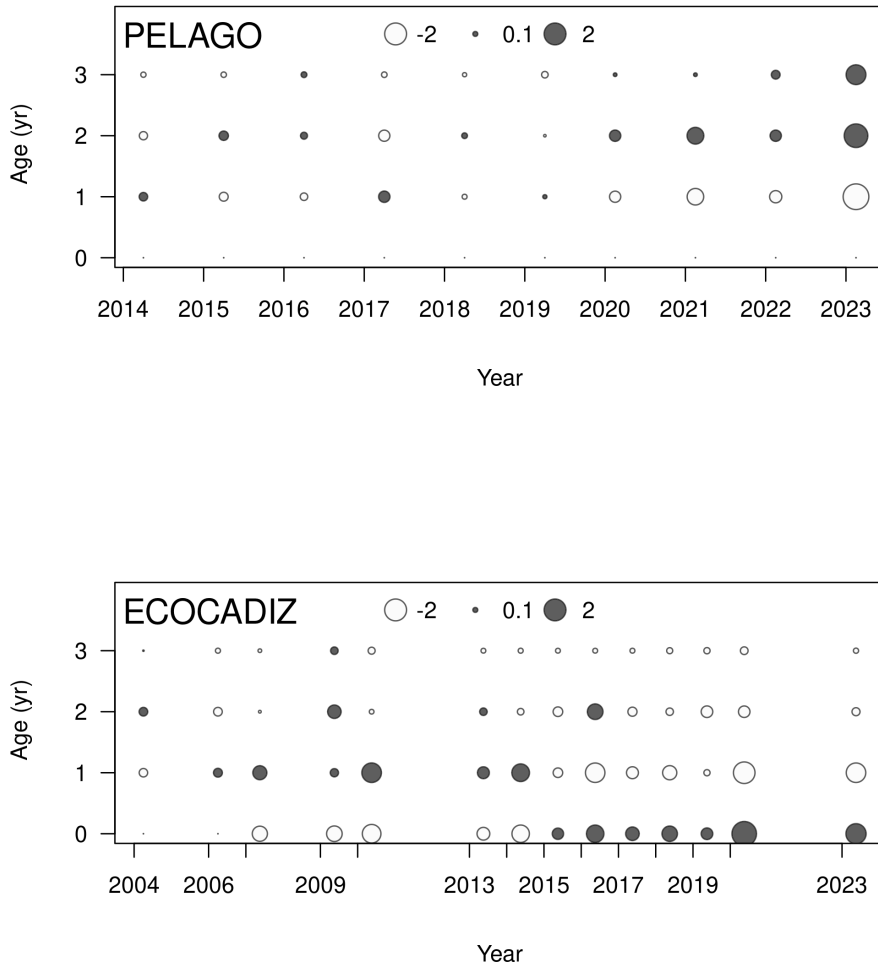


Figure 22: ane.27.9a Southern stock. Pearson residuals, comparing across surveys. Closed bubbles are positive residuals (observed > expected) and open negative residuals (observed < expected).

The Figure 23 shows that the residuals from the fit of the age proportions are randomly distributed, with p-values greater than 0.05 in the case of the commercial fleet (*SEINE*: ) and the acoustic surveys (*PELAGO*: 0.744, *ECOCADIZ-RECLUTAS*: 0.374). Some violations of the three-standard-deviation limit are observed for the commercial fleet (*SEINE*) during the fourth quarter of 1991, 1996, and 2012, as well as in the *PELAGO* survey in the last year of the series (2023). In the case of the *ECOCADIZ* survey, the residuals are not randomly distributed as indicated by a p-value of 0.014, with several violations of the three-standard-deviation limit observed, primarily from 2018 to 2023. The estimated root mean square error (RMSE) for the joint residual analysis is 29%.

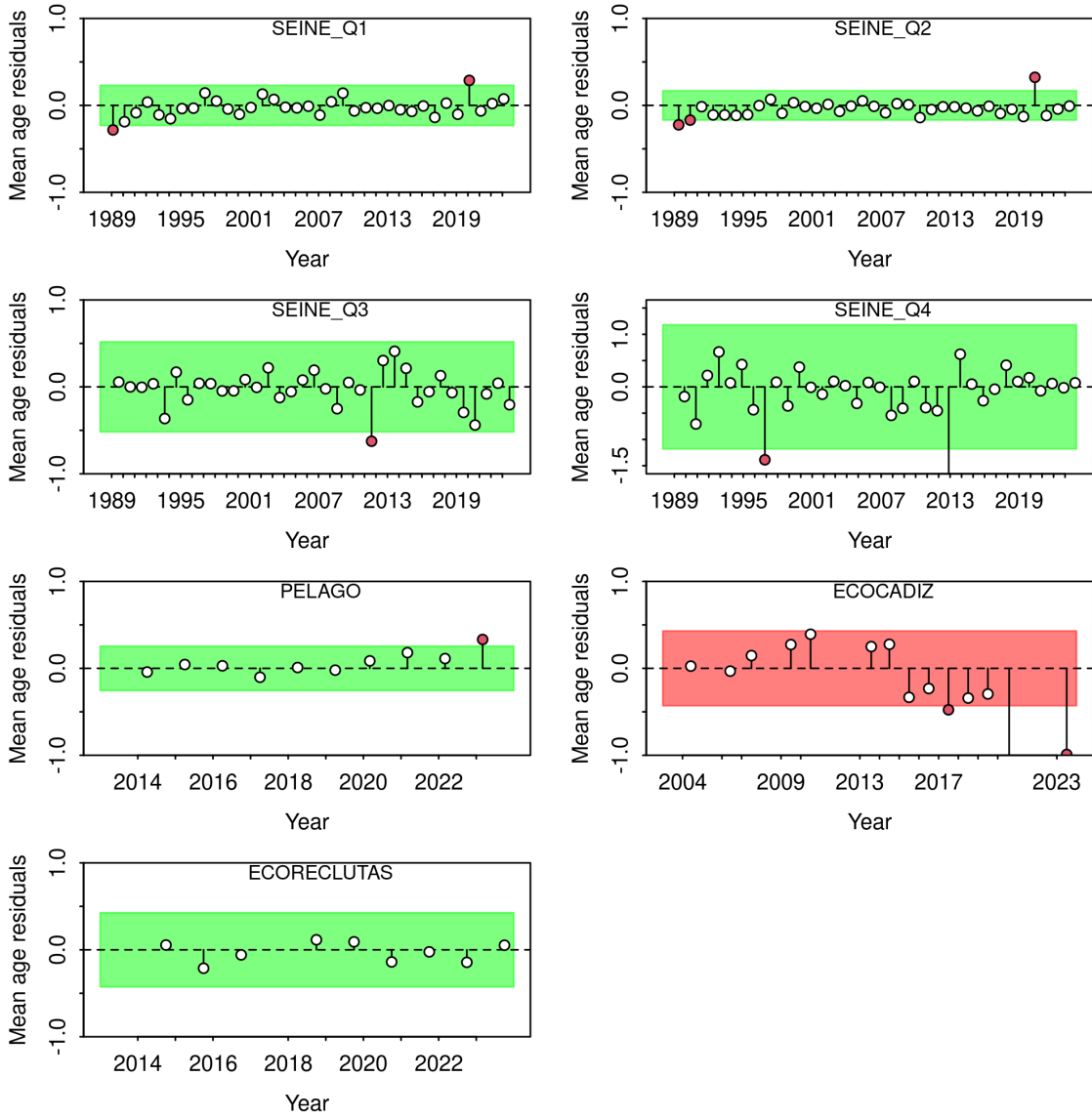


Figure 23: ane.27.9a Southern stock. a) Runs test results for fits to annual mean age estimates for the surveys (*PELAGO*, *ECOCADIZ*, *ECOCADIZ-RECLUTAS*) and the fishery (*SEINE*). Green shaded (green/red) area spans three residual standard deviations to either side from zero, and the red points outside of the shading violate the 'three-sigma limit' for that series. b) Joint residual plots for annual mean length estimates for surveys and fishery (bottom left panel). Vertical lines with points show the residuals, and the solid black line show loess smoother through all residuals. Root-mean squared error (RMSE) is included in the upper right-hand corner of the panel.

## Retrospective analysis

Figure 24 shows a retrospective pattern in both spawning biomass and fishing mortality in the base model. The retrospective analysis of the assessment model reveals that, in terms of Mohn's rho (mean of retrospective anomalies), the reduction in data leads to a pattern of underestimation in fishing mortality ( $\rho = -0.0703674$ ) and overestimation in spawning biomass ( $\rho = 0.0463587$ ). These Mohn's rho values were inside the bounds of recommended values, according to the rule proposed by Hurtado-Ferro *et al.* (2014), which states that

Mohn's rho index values should be less than 0.30 and greater than -0.22 for short-lived species.

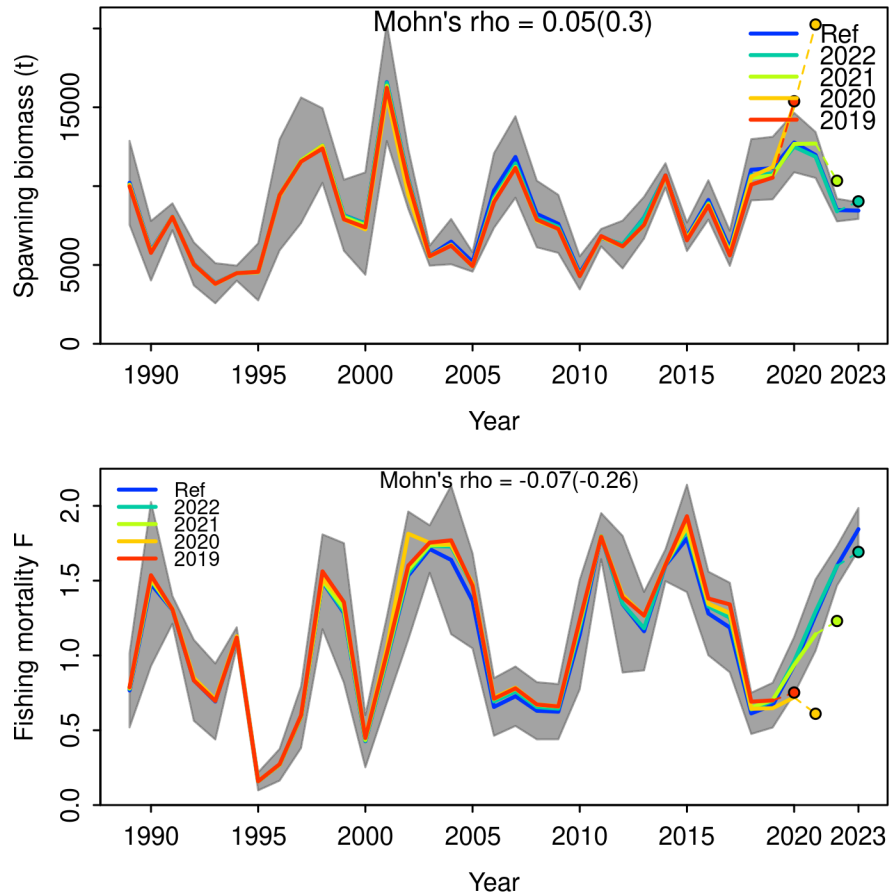


Figure 24: ane.27.9a Southern stock. Retrospective analysis of spawning stock biomass (SSB) and fishing mortality (F). Models conducted by re-fitting the reference model (Ref) after removing five years of observations, one year at a time sequentially. The retrospective results are shown the entire time series. Mohn's rho statistic and the corresponding 'hindcast rho' values (in brackets) are printed at the top of the panels. One-year-ahead projections denoted by color-coded dashed lines with terminal points are shown for each model. Grey shaded areas are the 95% confidence intervals from the reference model.

## Results

### Stock-recruitment relationship

Recruitment was modeled using a Beverton-Holt stock-recruitment relationship (Figure 25). The assumed level of underlying recruitment deviation error was fixed ( $\sigma_R=0.6$ ), equilibrium recruitment was estimated ( $\log(R_0)=15.54$ ) and steepness ( $h$ ) was fixed at 0.8.

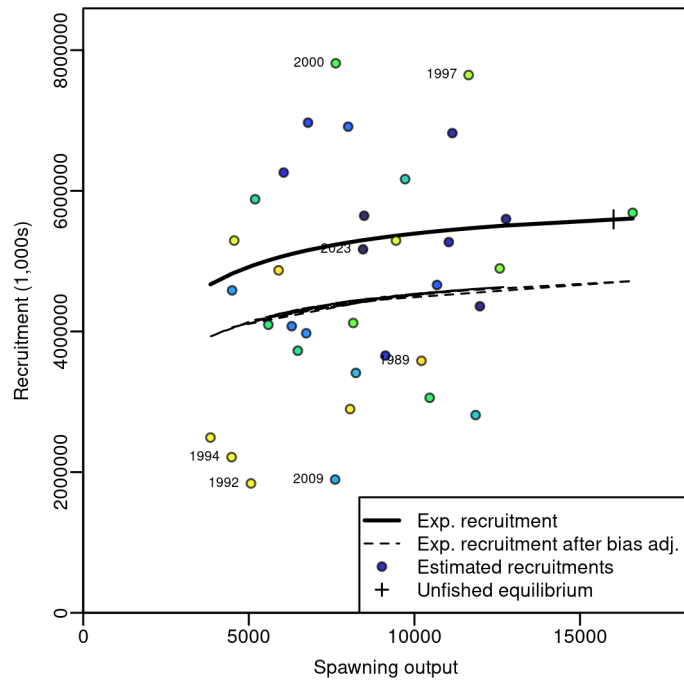


Figure 25: ane.27.9a Southern stock. Stock-recruit curve with labels on first, last, and years with (log) deviations  $> 0.5$ . Point colors indicate year, with warmer colors indicating earlier years and cooler colors in showing later years.

Recruitment deviations for the early (1985-1988) and main (1991-2023) periods in the model are presented in (Figure 26 ).

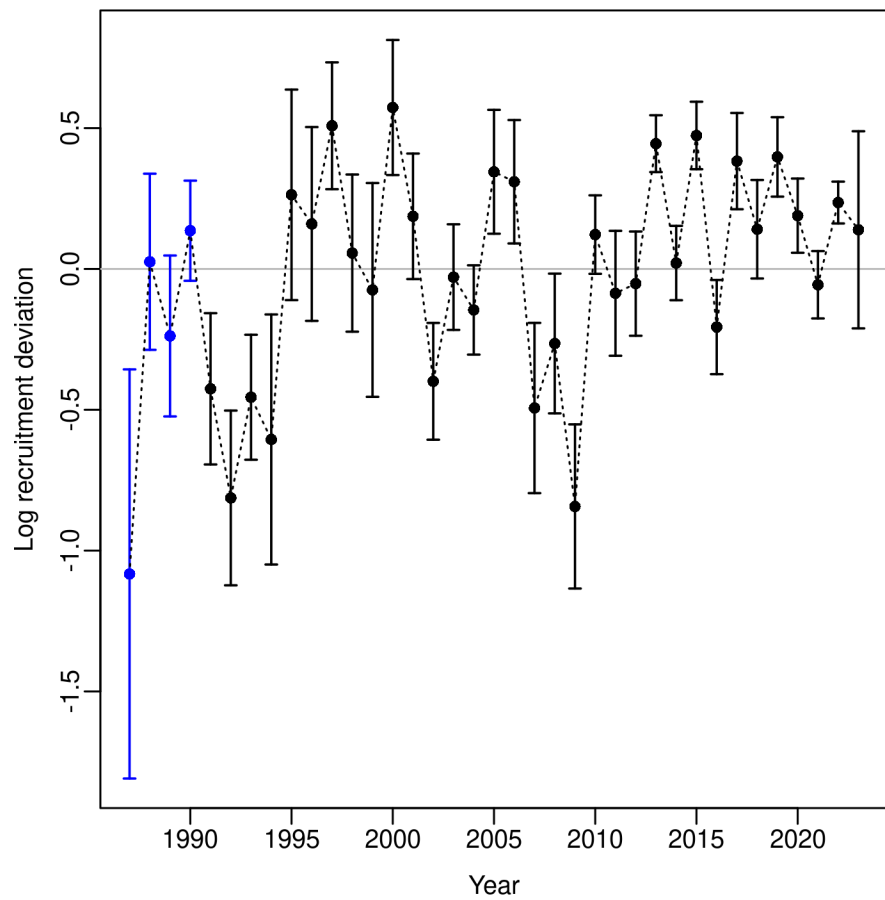


Figure 26: ane.27.9a Southern stock. Recruitment deviations with 95% intervals for the base model ( $\sigma_{\text{R}} = 0.3$  ).

Asymptotic standard errors for recruitment deviations are shown in Figure 27.

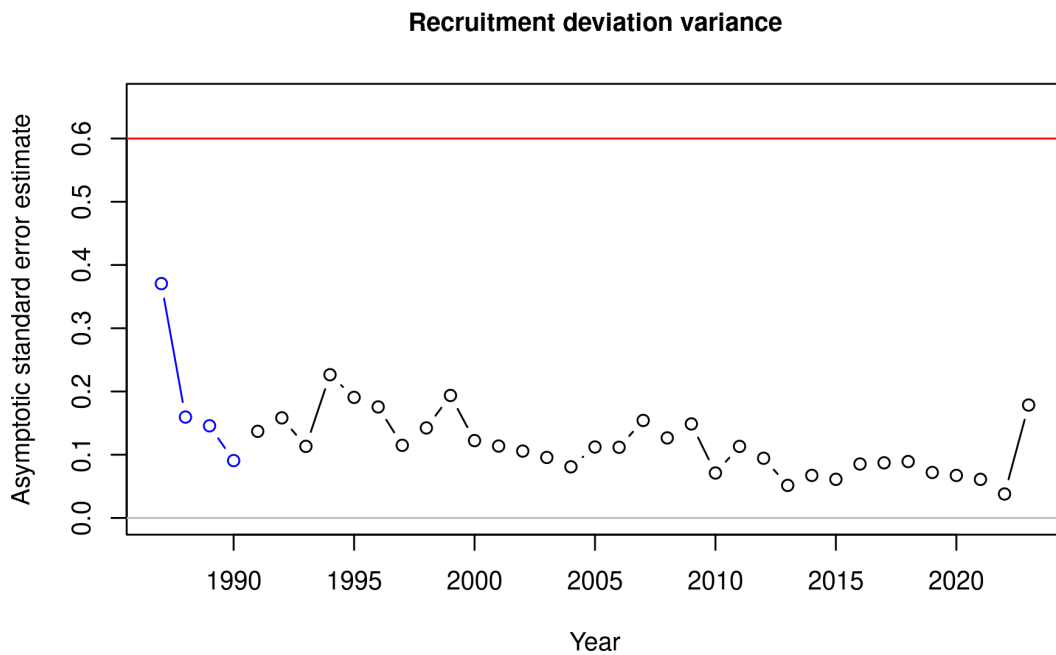


Figure 27: ane.27.9a Southern stock. Asymptotic standard errors for the estimated recruitment deviations.

Recruitment bias adjustment for the different periods is shown in Figure 28.

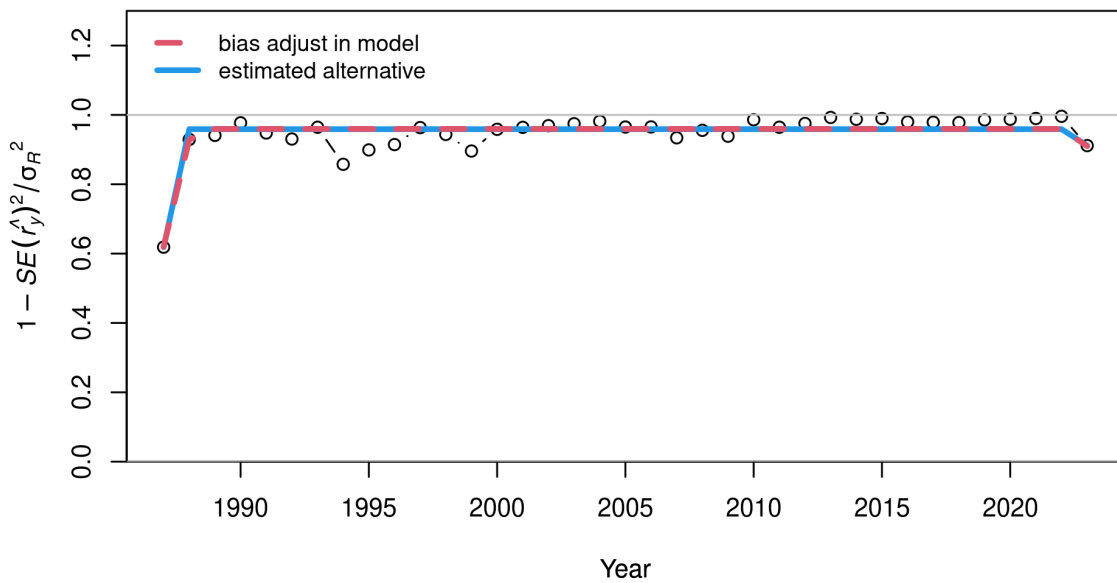


Figure 28: ane.27.9a Southern stock. Recruitment bias adjustment plot for early and main.

## Selectivity

Figure 29 shows the estimated selectivity for the age composition of the commercial fleet.

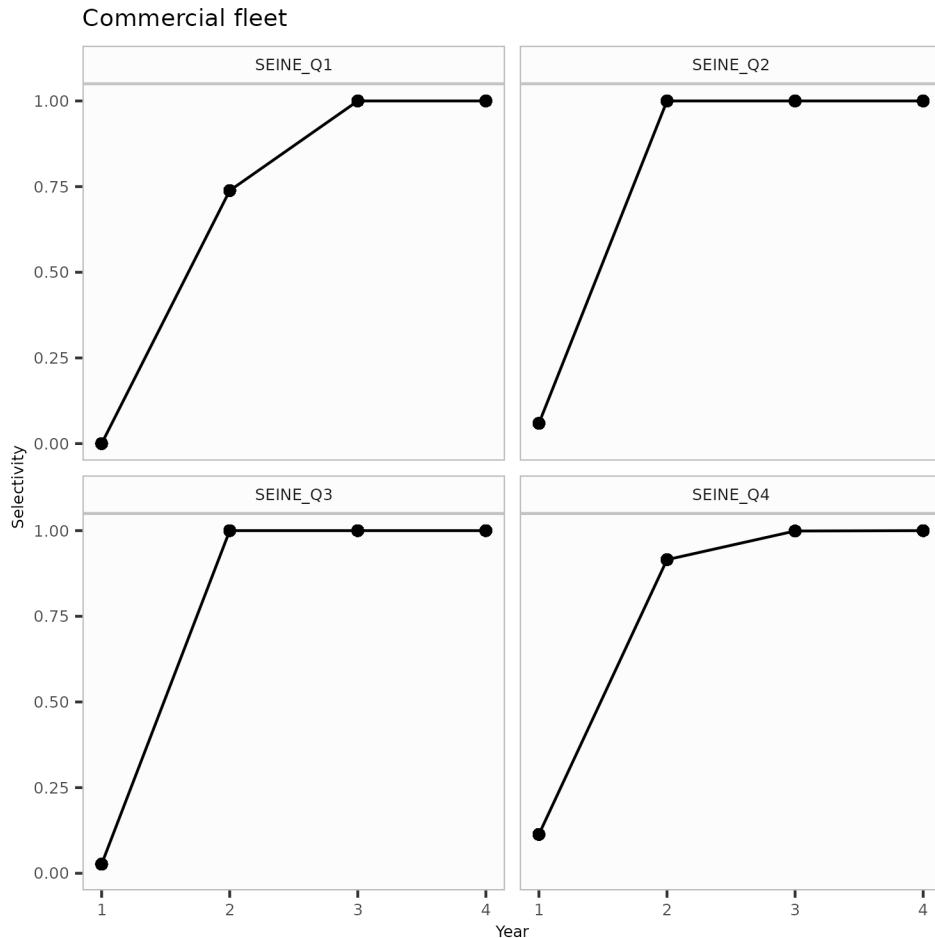


Figure 29: ane.27.9a Southern stock. Estimated selectivity for catch-at-age of commercial fleet (logistic shaped fixed selectivity across all years).

Figure 30 shows the estimated selectivity for the age composition of the acoustic surveys

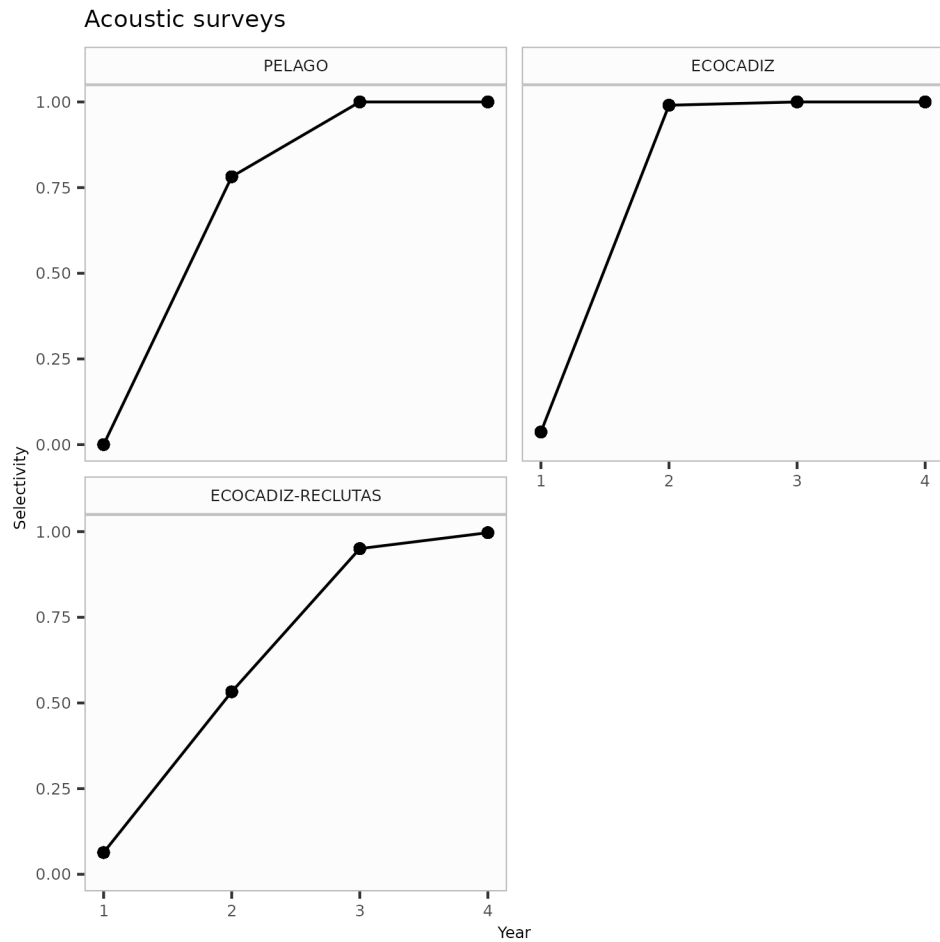


Figure 30: ane.27.9a Southern stock. Estimated selectivity for catch-at-age of surveys (logistic shaped fixed selectivity across all years)

But, it is important to remark that the selectivity assumption for *ECOCADIZ* survey was different from the others, and it was separated into two different periods: 2004 to 2014 and 2015 to 2023, this difference can be appreciated in Figure 31

## Catchability

The catchability ( $q$ ) is adjusted to maintain a consistent relationship between the observed biomass and the vulnerable biomass in acoustic surveys. As vulnerable biomass decreases throughout the year, catchability increases, indicating that efforts intensify when the vulnerable biomass is lower (Figure 31 ).

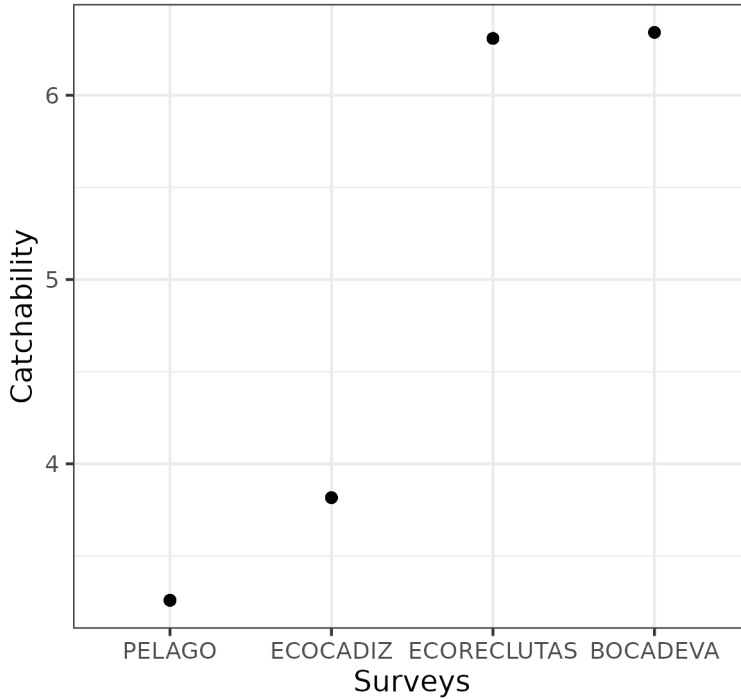


Figure 31: ane.27.9a Southern stock. Estimated catchability parameters for the different surveys indices.

### Estimated time series

The Figure 32 shows that total biomass fluctuates around a historical mean of 10.54 thousand tonnes, with a minimum in 1995 of 5.29 thousand tonnes and a maximum recorded in 2001 of 18.76 thousand tonnes. In 2023, the biomass is estimated to be -1% below the historical mean. The catch shows variability around the historical mean of 5.22 thousand tonnes, with a maximum value recorded in 1998 of 9.6 thousand tonnes and a minimum in 1995 of 0.57 thousand tonnes. In 2023, the catch is estimated to be 42% above the historical mean.

The fishing mortality ( $F_t$ ) fluctuates around a historical mean of 1.1, with a maximum value recorded in 2023 of 1.84 and a minimum in 1995 of 0.16. Confidence intervals range from 0.21 to 0.03, with an average of 0.13. The  $F_{2023}$  is estimated to be 68% above the historical mean.

The recruitment ( $R_t$ ) fluctuates around a historical mean of 4.68 millions recruits, with a maximum value recorded in 2000 of 7.81 millions recruits and a minimum in 1992 of 1.84 millions recruits. Confidence intervals range from 0.23 to 0.03, with an average of 0.11. The  $R_{2023}$  is estimated to be -11% below the historical mean.

Finally, the spawning biomass ( $SSB_t$ ) varies around a historical mean of 8.44 thousand tonnes, with a maximum value recorded in 2001 of 16.59 thousand tonnes and a minimum in 1993 of 3.84 thousand tonnes. Confidence intervals range from 0.22 to 0.03, with an average of 0.11. The  $SSB_{2023}$  is estimated to be 0% below the historical mean.

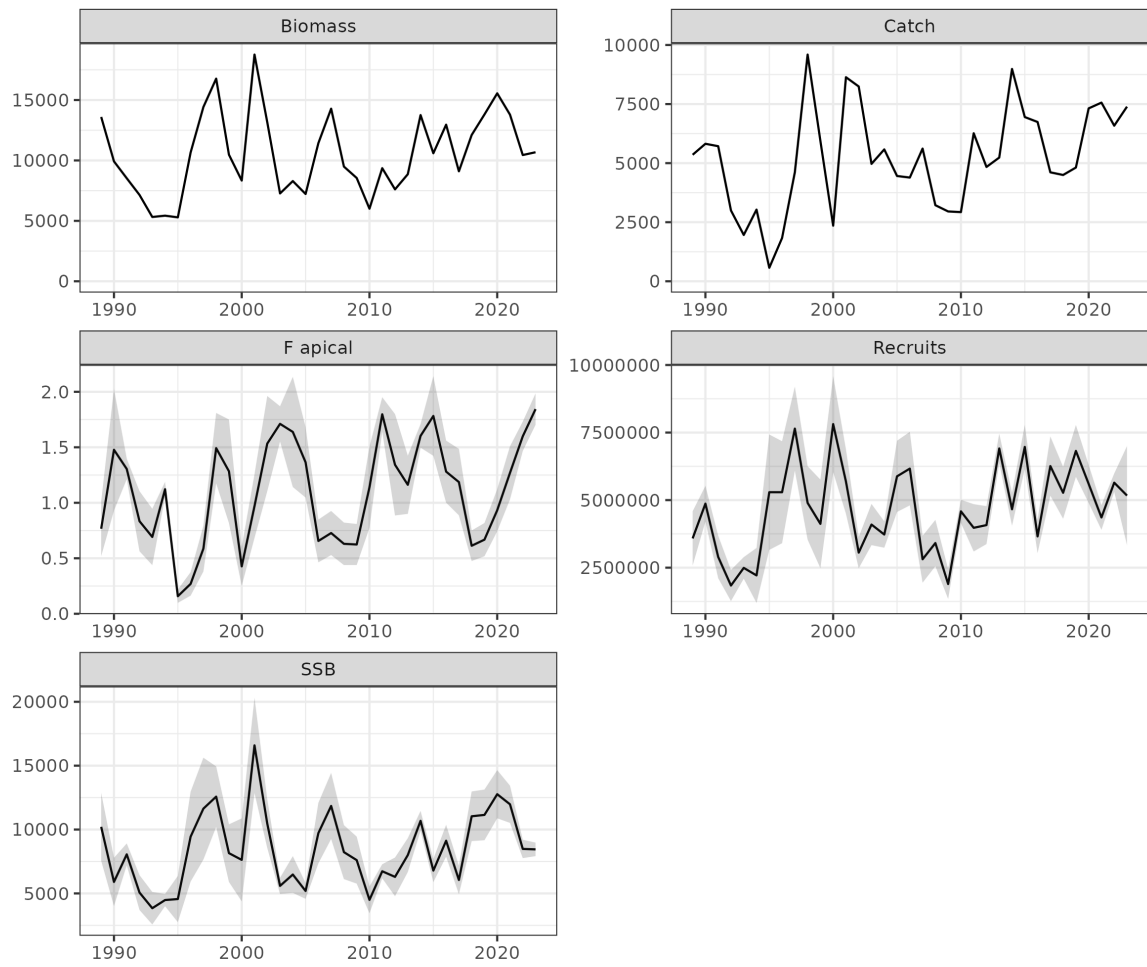


Figure 32: ane.27.9a Southern stock. Time series estimated by the model for annual catches (in tons), recruitment (millions of fish), total biomass and spawning biomass (in tons), and fishing mortality (year-1).

The summarised data resulting from model outputs is shown in Figure 33.

Year	SSB ton	CV SSB	Recruits number	CV Recruits	F apical year-1	CV F apical	Total Biomass ton	Catch ton
1989	10211.80	0.13	3582960	0.14	0.77	0.16	13600.60	5354.25
1990	5899.18	0.16	4869320	0.07	1.48	0.19	9923.34	5819.06
1991	8058.54	0.05	2896830	0.14	1.30	0.04	8526.07	5716.59
1992	5065.71	0.14	1839190	0.16	0.83	0.17	7145.64	2996.70
1993	3842.34	0.17	2491640	0.08	0.69	0.19	5320.99	1959.95
1994	4480.87	0.05	2213260	0.23	1.12	0.03	5428.81	3033.07
1995	4559.73	0.20	5292860	0.21	0.16	0.19	5289.70	570.61
1996	9443.32	0.19	5292120	0.18	0.27	0.20	10658.30	1831.41
1997	11636.20	0.17	7645870	0.10	0.59	0.18	14420.90	4613.21
1998	12575.30	0.10	4895920	0.14	1.49	0.11	16770.60	9595.06
1999	8152.42	0.14	4120750	0.20	1.28	0.19	10476.60	5940.55
2000	7624.81	0.22	7812990	0.12	0.43	0.21	8335.88	2353.44
2001	16589.80	0.11	5686770	0.11	0.97	0.15	18762.70	8636.66
2002	10460.60	0.09	3057050	0.10	1.53	0.14	13160.00	8244.26
2003	5589.69	0.06	4095540	0.09	1.71	0.05	7269.35	4969.11
2004	6479.28	0.11	3726440	0.07	1.64	0.15	8292.85	5581.19
2005	5190.29	0.06	5879900	0.11	1.36	0.12	7223.30	4455.43
2006	9719.44	0.12	6165750	0.11	0.66	0.15	11430.90	4389.09
2007	11847.80	0.11	2811110	0.16	0.73	0.14	14285.20	5616.24
2008	8231.44	0.13	3410900	0.13	0.63	0.15	9491.18	3219.63
2009	7606.14	0.12	1894580	0.15	0.62	0.15	8547.92	2954.92
2010	4495.79	0.12	4584240	0.05	1.14	0.16	6006.05	2927.42
2011	6733.35	0.04	3974710	0.11	1.80	0.04	9359.67	6264.97
2012	6295.65	0.12	4074870	0.09	1.34	0.17	7605.90	4838.20
2013	7999.69	0.08	6911620	0.04	1.16	0.12	8860.52	5235.86
2014	10681.60	0.04	4661330	0.07	1.60	0.03	13754.70	8986.11
2015	6787.52	0.07	6968740	0.06	1.78	0.10	10594.40	6950.09
2016	9124.41	0.07	3656740	0.09	1.28	0.11	12960.00	6741.82
2017	6053.20	0.09	6259490	0.09	1.19	0.13	9101.95	4610.86
2018	11037.80	0.09	5271280	0.09	0.61	0.11	12106.10	4498.81
2019	11145.60	0.09	6820340	0.07	0.67	0.11	13804.70	4813.58
2020	12765.60	0.08	5598630	0.06	0.93	0.10	15555.00	7317.35
2021	11976.20	0.06	4358380	0.05	1.27	0.10	13789.60	7561.60
2022	8482.40	0.04	5645520	0.03	1.60	0.04	10447.90	6585.17
2023	8448.08	0.03	5168160	0.18	1.84	0.04	10679.20	7390.68

Figure 33: ane.27.9a Southern stock. Time series estimated by the model for annual catches (in tons), recruitment (millions of fish), total biomass and spawning biomass (in tons), and fishing mortality (year-1).

## Acknowledgements

Financial support was received for the work developed in this document. In particular, M. José Zúñiga work was funded by the Math4Fish project: New tools for mathematical modelling in Spanish fisheries scientific advice, financed by the European Union – NextGenerationEU, and the Recovery and Resilience Facility, Component 3, Investment 7 and has been carried out within the framework of the agreement between the Spanish Ministry of Agriculture, Fishing and Food and the Spanish National Research Council (CSIC) through the Spanish Institute of Oceanography (IEO) to promote fisheries research as a basis for sustainable fisheries management. Views and opinions expressed are however those of the author(s) only and do not

necessarily reflect those of the European Union or European Commission. Neither the European Union nor the European Commission can be held responsible for them.

Additionally, this work would have not been possible without the collection of Spanish fisheries and surveys data, co-funded by the Spanish Institute of Oceanography (IEO) and the EU through the European Maritime and Fisheries Fund (EMFF) within the National Program of collection, management and use of data in the fisheries sector and support for scientific advice regarding the Common Fisheries Policy (PNDB/EU-DCF-Programa Nacional de Datos Básicos/EU-Data Collection Framework).

## References

- Carvalho, F., Winker, H., Courtney, D., Kapur, M., Kell, L., Cardinale, M., Schirripa, M., *et al.* 2021. A cookbook for using model diagnostics in integrated stock assessments. *Fisheries Research*, 240: 105959. <https://www.sciencedirect.com/science/article/pii/S0165783621000874>.
- Francis, R. I. C. C. 2011. Data weighting in statistical fisheries stock assessment models. *Canadian Journal of Fisheries and Aquatic Sciences*, 68: 1124–1138. <https://doi.org/10.1139/f2011-025>.
- Hsu, J., Chang, Y.-J., Brodziak, J., Kai, M., and Punt, A. E. 2024. On the probable distribution of stock-recruitment resilience of Pacific saury (*Cololabis saira*) in the Northwest Pacific Ocean. *ICES Journal of Marine Science*, 81: 748–759. <https://doi.org/10.1093/icesjms/fsae030>.
- Hurtado-Ferro, F., Szuwalski, C. S., Valero, J. L., Anderson, S. C., Cunningham, C. J., Johnson, K. F., Licandeo, R., *et al.* 2014. Looking in the rear-view mirror: bias and retrospective patterns in integrated, age-structured stock assessment models. *ICES Journal of Marine Science*, 72: 99–110. <https://doi.org/10.1093/icesjms/fsu198>.
- Methot, R. D., and Taylor, I. G. 2011. Adjusting for bias due to variability of estimated recruitments in fishery assessment models. *Canadian Journal of Fisheries and Aquatic Sciences*, 68: 1744–1760. <https://doi.org/10.1139/f2011-092>.
- Methot, R. D., and Wetzel, C. R. 2013. Stock synthesis: A biological and statistical framework for fish stock assessment and fishery management. *Fisheries Research*, 142: 86–99. <https://doi.org/10.1016/j.fishres.2012.10.012>.
- Methot, R. D., Wetzel, C. R., Taylor, I. G., Doering, K., Perl, E., and K. Johnson. 2024. Stock synthesis user manual : Version 3.30.22.1. <https://github.com/nmfs-ost/ss3-source-code/releases>.
- Taylor, I. G., Doering, K. L., Johnson, K. F., Wetzel, C. R., and Stewart, I. J. 2021. Beyond visualizing catch-at-age models: Lessons learned from the r4ss package about software to support stock assessments. *Fisheries Research*, 239: 105924. <https://doi.org/10.1016/j.fishres.2021.105924>.
- Wiff, R., Flores, A., Neira, S., and Caneco, B. 2018. Estimating steepness of the stock-recruitment relationship in chilean fish stocks using meta-analysis. *Fisheries Research*, 200: 61–67. <https://www.sciencedirect.com/science/article/pii/S0165783617303399>.